



PONTIFICIA
**UNIVERSIDAD
CATÓLICA**
DEL PERÚ

th
TECHNISCHE UNIVERSITÄT
ILMENAU

Pontificia Universidad Católica del Perú

Escuela de Posgrado

Tesis

A Theoretical Model of a Laboratory-Scale Ethanol Distillation Column

Para optar el grado académico de
Magíster en Ingeniería de Control y Automatización

Presentado por:
Ing. Maria Fernanda Aguinaga Morón

Profesor Responsable (TU Ilmenau): Univ.-Prof. Dr. Yuri Andri Shardt Wolchuk

Profesor Responsable (PUCP): Dr. Ing. Juan Javier Sotomayor Moriano

Febrero, 2021

Resumen

En la producción química moderna, los procesos de destilación son frecuentemente utilizados como método de separación de líquidos. Modelar una columna de destilación nos permite predecir el comportamiento del sistema. El modelado de sistemas es una importante, y sin embargo a veces descuidada, disciplina de la ingeniería de control. Esta tesis de maestría se centra en el modelado de la columna de destilación a escala de laboratorio situada en el Instituto de automatización de la Universidad técnica de Ilmenau. Esta columna, utilizada principalmente para la enseñanza y la investigación, separa el etanol y el agua en diez etapas. El modelo teórico del sistema se realiza utilizando el modelo de primeros principios (FPM), principalmente las ecuaciones MESH para representar las ecuaciones altamente no lineales, que incluyen el equilibrio de masa, las relaciones de fase de equilibrio, las ecuaciones de sumatoria y el equilibrio de energía para cada etapa. Para ilustrar cómo se comporta el modelo de la columna de destilación, este trabajo presenta simulaciones de las concentraciones por etapa y de la temperatura a lo largo de la columna. Así mismo, los resultados se comparan con el modelo de McCabe-Thiele y con temperaturas experimentales lo cual muestra buenos resultados. En el caso de la comparación con McCabe-Thiele, ambas fracciones molares líquidas $x_{1McT} = 0.035$ mol/mol y $x_{1Sim} = 0.048$ mol/mol son más pequeñas que la requerida $x_B = 0.1$, el error es dado porque las concentraciones en las etapas iniciales son más influenciadas por las suposiciones de la alimentación y las condiciones iniciales de la columna. Sin embargo, para el tope de la columna las fracciones molares finales son $x_{10McT} = 0.885$ mol/mol y $x_{10Sim} = 0.890$ mol/mol, valores mucho más cercanos al requerido $x_D = 0.9$. Para las fracciones molares de vapor, $y_{1McT} = 0.334$ mol/mol y $y_{1Sim} = 0.384$ mol/mol se diferencian en 14% dado que no tienen un punto de inicio compartido. Sin embargo, más importante, para el tope de la columna las fracciones molares finales son $y_{10McT} = 0.901$ mol/mol y $y_{10Sim} = 0.9060$ mol/mol, y el promedio del error en la totalidad de la columna es de $\mu_{error} = 0.0028$ para los datos disponibles. En el caso de la comparación contra la temperatura experimental, los errores más grandes se encontraron en las etapas del medio, como era esperado, debido a que la temperatura de la alimentación (etapa 5) afecta esa etapa y las cercanas a esta. Sin embargo, esto no afectará los resultados generales de la simulación dado que las temperaturas finales para el fondo de la columna son $T_{f1Mod} = 85.6^\circ\text{C}$ y $T_{f1Exp} = 85.8^\circ\text{C}$. Y para el tope de la columna, $T_{f10Mod} = 78.5^\circ\text{C}$ y $T_{f10Exp} = 78.7^\circ\text{C}$, ambos más altos que el punto de ebullición del ethanol y más bajos que el punto de ebullición del agua. Para mejorar las simulaciones, habría que hacer más experimentos en la planta utilizando un cromatógrafo de gases y sensores de temperatura y presión.



TECHNISCHE UNIVERSITÄT
ILMENAU

TECHNISCHE UNIVERSITÄT ILMENAU
FACULTY OF COMPUTER SCIENCE AND AUTOMATION

Master's Thesis

A Theoretical Model of a Laboratory-Scale Ethanol Distillation Column

Submitted by: Ing. Maria Fernanda Aguinaga Morón

Date and place of birth: 1990/07/20 in Lima, Peru

Degree Programme: Technische Kybernetik und Systemtheorie

Matriculation Number: 61323

Supervisor TU-Ilmenau: Univ.-Prof. Dr. Yuri Andri Wolchuk Shardt

Supervisor PUCP: Dr. Ing. Juan Javier Sotomayor Moriano

Submitted on: 2021/02/22

Selbständigkeitsklärung

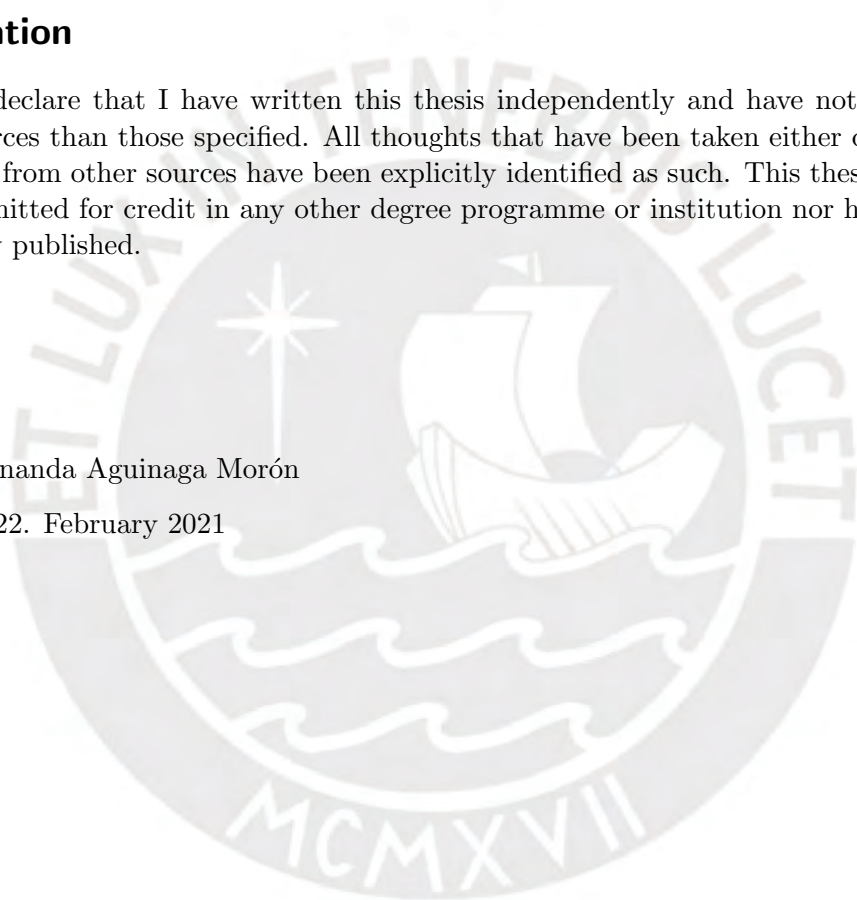
Ich erkläre hiermit, daß ich die vorliegende Arbeit selbständig verfaßt und keine anderen als die angegebenen Quellen benutzt habe. Alle Gedanken, die aus fremden Quellen direkt oder indirekt übernommenen wurden, sind als solche kenntlich gemacht. Die Arbeit wurde bisher keiner anderen Prüfungsbehörde vorgelegt und auch noch nicht veröffentlicht.

Declaration

I hereby declare that I have written this thesis independently and have not used any other sources than those specified. All thoughts that have been taken either directly or indirectly from other sources have been explicitly identified as such. This thesis has not been submitted for credit in any other degree programme or institution nor has it been previously published.

Maria Fernanda Aguinaga Morón

Ilmenau, 22. February 2021



Acknowledgements

I deeply thank my mother, for the freedom; for educating me, loving me and supporting me in every endeavor.

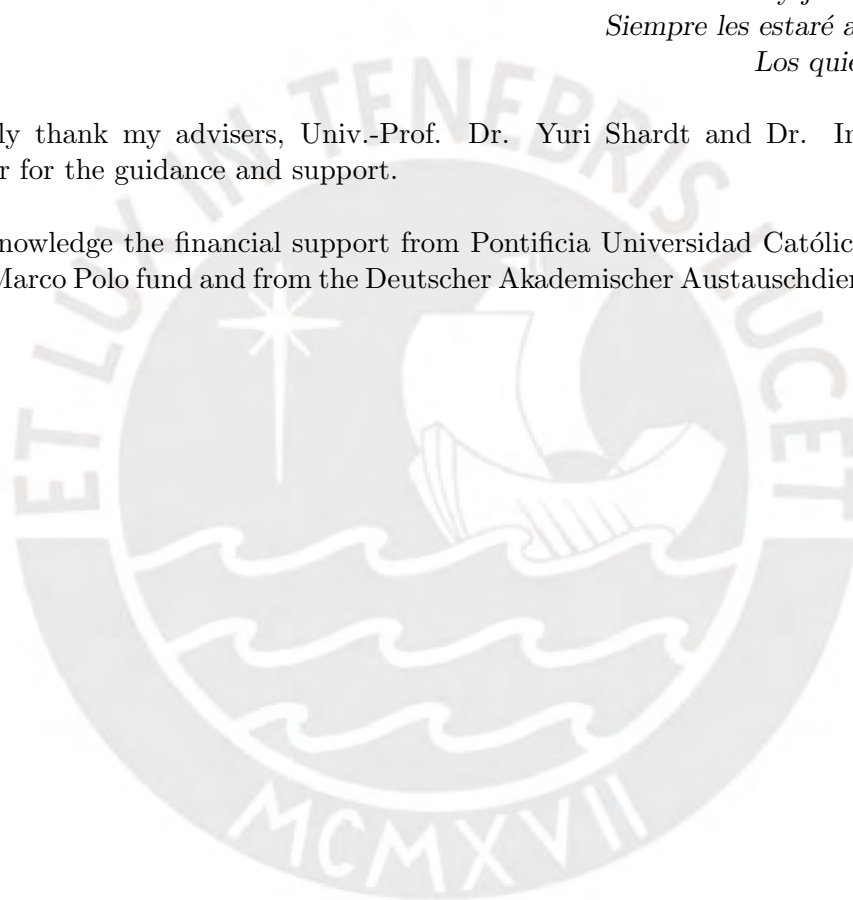
Por ti, esto es posible.

To my grandmother and grandfather, Lucho and Yoli.

*A él, por ser la fuerza
que me impulsa a ser mejor.
Gracias a ella que un día
tomó mi mano y jamás la soltó.
Siempre les estaré agradecida.
Los quiero mucho.*

I gratefully thank my advisers, Univ.-Prof. Dr. Yuri Shardt and Dr. Ing. Javier Sotomayor for the guidance and support.

I also acknowledge the financial support from Pontificia Universidad Católica del Perú (PUCP) Marco Polo fund and from the Deutscher Akademischer Austauschdienst (DAAD).



Abstract

In modern chemical production, distillation processes are often used for liquid separation. Modeling a distillation column allows us to predict the system's behavior. System modeling is an important, and yet sometimes neglected, discipline of control engineering. This master's thesis is focused on modeling the laboratory-scale distillation column located in the Institute of Automation and Systems Engineering at the Technical University of Ilmenau. This column, mainly used for teaching and research, separates ethanol and water in ten stages. The theoretical model of the system is found using a first principle model (**FPM**), mainly the MESH equations to present the highly nonlinear equations, that include the mass balance, the equilibrium phase relationships, the summation equations, and the energy balance for each stage, resulting in the differential equations of the system dynamics. To illustrate how the model of the distillation column behaves, this work presents the simulations of the concentrations per stage and of the temperature along the column. As well, the results are compared with the McCabe-Thiele model of the system and with experimental temperatures which show good results. In the case of the comparison with McCabe-Thiele, both initial liquid mole fractions $x_{1McT} = 0.035$ mol/mol and $x_{1Sim} = 0.048$ mol/mol are smaller than the required $x_B = 0.1$, the present error is because the concentrations in the initial stages is mostly influenced by the assumptions of the feed concentration and initial conditions of the column. However, for the top of the column the final mole fractions are $x_{10McT} = 0.885$ mol/mol and $x_{10Sim} = 0.890$ mol/mol, values that are much closer to the required value of $x_D = 0.9$. For the vapor mole fractions, $y_{1McT} = 0.334$ mol/mol and $y_{1Sim} = 0.384$ mol/mol differ in 14% since there is no shared starting point. However, more importantly, for the top of the column the final mole fractions are $y_{10McT} = 0.901$ mol/mol and $y_{10Sim} = 0.9060$ mol/mol, and the mean of the error along the column is $\mu_{error} = 0.0028$ for the available data. In the case of the temperature comparison of the model against experimental available data, the bigger errors in the temperature were given in the middle stages, as expected, since the temperature of the feed (in stage 5) affects that stage and the ones above and below it. However, this will not affect the overall simulation results since the final temperatures for the bottom tray are $T_{f1Mod} = 85.6^\circ\text{C}$ and $T_{f1Exp} = 85.8^\circ\text{C}$. And for the top tray, $T_{f10Mod} = 78.5^\circ\text{C}$ and $T_{f10Exp} = 78.7^\circ\text{C}$, both higher than the ethanol boiling point and lower than the water boiling point. In order to improve the simulations, more experiments should be made in the plant using a gas chromatograph and temperature and pressure sensors.

Resumen

En la producción química moderna, los procesos de destilación son frecuentemente utilizados como método de separación de líquidos. Modelar una columna de destilación nos permite predecir el comportamiento del sistema. El modelado de sistemas es una importante, y sin embargo a veces descuidada, disciplina de la ingeniería de control. Esta tesis de maestría se centra en el modelado de la columna de destilación a escala de laboratorio situada en el Instituto de automatización de la Universidad técnica de Ilmenau. Esta columna, utilizada principalmente para la enseñanza y la investigación, separa el etanol y el agua en diez etapas. El modelo teórico del sistema se realiza utilizando el modelo de primeros principios (FPM), principalmente las ecuaciones MESH para representar las ecuaciones altamente no lineales, que incluyen el equilibrio de masa, las relaciones de fase de equilibrio, las ecuaciones de sumatoria y el equilibrio de energía para cada etapa. Para ilustrar cómo se comporta el modelo de la columna de destilación, este trabajo presenta simulaciones de las concentraciones por etapa y de la temperatura a lo largo de la columna. Así mismo, los resultados se comparan con el modelo de McCabe-Thiele y con temperaturas experimentales lo cual muestra buenos resultados. En el caso de la comparación con McCabe-Thiele, ambas fracciones molares líquidas $x_{1McT} = 0.035$ mol/mol y $x_{1Sim} = 0.048$ mol/mol son más pequeñas que la requerida $x_B = 0.1$, el error es dado porque las concentraciones en las etapas iniciales son más influenciadas por las suposiciones de la alimentación y las condiciones iniciales de la columna. Sin embargo, para el tope de la columna las fracciones molares finales son $x_{10McT} = 0.885$ mol/mol y $x_{10Sim} = 0.890$ mol/mol, valores mucho más cercanos al requerido $x_D = 0.9$. Para las fracciones molares de vapor, $y_{1McT} = 0.334$ mol/mol y $y_{1Sim} = 0.384$ mol/mol se diferencian en 14% dado que no tienen un punto de inicio compartido. Sin embargo, más importante, para el tope de la columna las fracciones molares finales son $y_{10McT} = 0.901$ mol/mol y $y_{10Sim} = 0.9060$ mol/mol, y el promedio del error en la totalidad de la columna es de $\mu_{error} = 0.0028$ para los datos disponibles. En el caso de la comparación contra la temperatura experimental, los errores más grandes se encontraron en las etapas del medio, como era esperado, debido a que la temperatura de la alimentación (etapa 5) afecta esa etapa y las cercanas a esta. Sin embargo, esto no afectará los resultados generales de la simulación dado que las temperaturas finales para el fondo de la columna son $T_{f1Mod} = 85.6^\circ\text{C}$ y $T_{f1Exp} = 85.8^\circ\text{C}$. Y para el tope de la columna, $T_{f10Mod} = 78.5^\circ\text{C}$ y $T_{f10Exp} = 78.7^\circ\text{C}$, ambos más altos que el punto de ebullición del ethanol y más bajos que el punto de ebullición del agua. Para mejorar las simulaciones, habría que hacer más experimentos en la planta utilizando un cromatógrafo de gases y sensores de temperatura y presión.

Kurzfassung

In der modernen chemischen Produktion werden Destillationsprozesse häufig als Methode zur Flüssigkeitstrennung eingesetzt. Die Modellierung einer Destillationskolonne ermöglicht die Vorhersage des Systemverhaltens. Systemmodellierung ist eine wichtige, aber manchmal vernachlässigte Disziplin der Regelungstechnik. Diese Masterarbeit beschäftigt sich mit der Modellierung der Destillationskolonne im Labormaßstab, die sich im Institut Automatisierungs- und Systemtechnik der Technischen Universität Ilmenau befindet. Diese Kolonne, die meistens zu Lehr- und Forschungszwecken eingesetzt wird, trennt Ethanol und Wasser in zehn Stufen. Das theoretische Modell des Systems wird unter Verwendung des ab-initio-Modellen (FPM) erstellt, hauptsächlich der MESH-Gleichungen zur Darstellung der hochgradig nichtlinearen Gleichungen, die die Massenbilanz, die Gleichgewichtsphasenbeziehungen, die Summationsgleichungen und die Energiebilanz für jede Stufe umfassen. Um zu veranschaulichen, wie sich das Modell der Destillationskolonne verhält, werden in dieser Masterarbeit Simulationen der Konzentrationen pro Stufe und der Temperatur entlang der Kolonne vorgestellt. Außerdem werden die Ergebnisse mit dem McCabe-Thiele-Modell des Systems und mit experimentellen Temperaturen verglichen, die gute Ergebnisse zeigen. Beim Vergleich mit McCabe-Thiele sind beide anfänglichen Flüssigkeitsmolanteile $x_{1McT} = 0.035$ mol/mol und $x_{1Sim} = 0.048$ mol/mol kleiner als die geforderte $x_B = 0.1$, der vorliegende Fehler ist darauf zurückzuführen, dass die Konzentrationen in den Anfangsstufen hauptsächlich von den Annahmen der Zulaufkonzentration und den Anfangsbedingungen der Kolonne beeinflusst werden. Für den Kopf der Kolonne betragen die endgültigen Molfraktionen jedoch $x_{10McT} = 0,885$ mol/mol und $x_{10Sim} = 0,890$ mol/mol, Werte, die viel näher am erforderlichen Wert von $x_D = 0,9$ liegen. Für die Dampfanteile $y_{1McT} = 0.334$ mol/mol und $y_{1Sim} = 0.384$ mol/mol unterscheiden sich um 14%, da es keinen gemeinsamen Startpunkt gibt. Wichtiger ist jedoch, dass für den oberen Teil der Säule die endgültigen Molenbrüche $y_{10McT} = 0.901$ mol/mol und $y_{10Sim} = 0.9060$ mol/mol sind und der Mittelwert des Fehlers entlang der Säule $\mu_{error} = 0.0028$ für die verfügbaren Daten ist. Beim Temperaturvergleich des Modells mit den verfügbaren experimentellen Daten wurden die größeren Fehler bei der Temperatur in den mittleren Stufen angegeben, wie erwartet, da die Temperatur des Vorschubs (in Stufe 5) diese Stufe und die darüber und darunter liegenden beeinflusst. Dies hat jedoch keinen Einfluss auf die Gesamtsimulationsergebnisse, da die Endtemperaturen für die untere Schale $T_{f1Mod} = 85.6^\circ\text{C}$ und $T_{f1Exp} = 85.8^\circ\text{C}$ sind. Und für die obere Schale sind $T_{f10Mod} = 78,5^\circ\text{C}$ und $T_{f10Exp} = 78,7^\circ\text{C}$, beide höher als der Ethanol-Siedepunkt und niedriger als der Wasser-Siedepunkt. Um die Simulationen zu verbessern, sollten weitere Versuche in der Anlage

mit einem Gaschromatographen und Temperatur- und Drucksensoren durchgeführt werden.

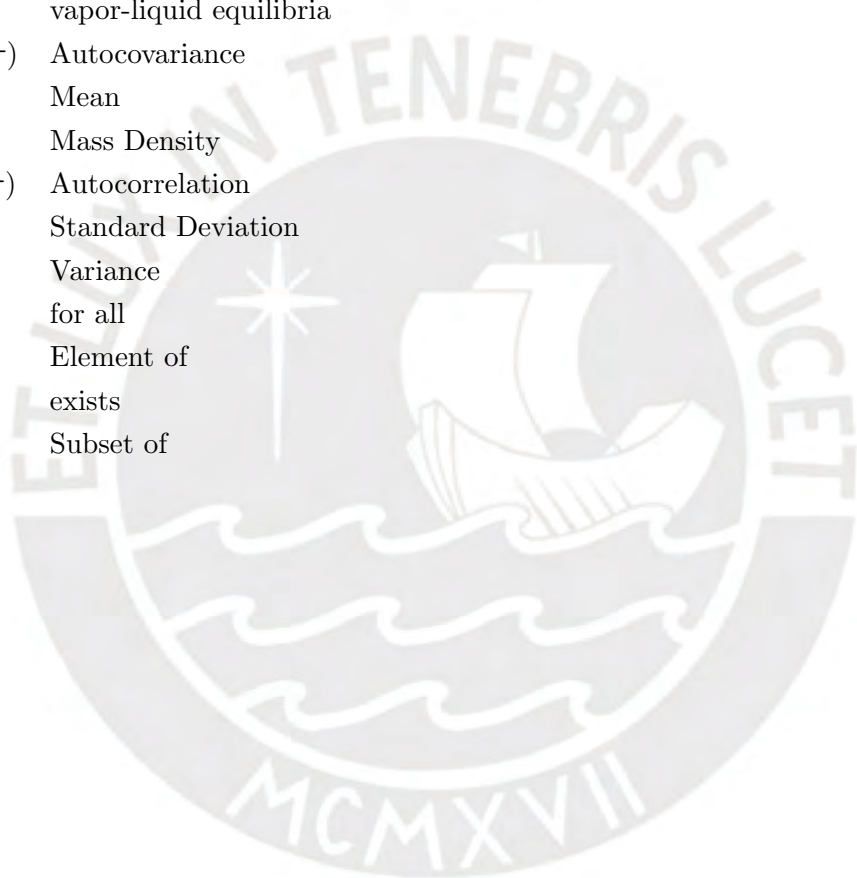


Notation

A	Regression Matrix
B	Bottoms or Raffinate
b	Molar Availabilities
C	Heat Capacity Constant
c	Molar Concentration [kmol/m ³]
D	Distillate
E	Expectation Operator
F	Molar Flow rate of Feed [kmol/s]
f	Feed plate subscript
f^{nExp}	Final Experimental Temperature in the Stage n subscript
f^{nMod}	Final Modeled Temperature in the Stage n subscript
H	Enthalpy, or Henry's law constant [Pa/mol]
h	Molar Enthalpies
K	K-value or Vapor-Liquid Equilibrium ratio
K_{ji}	Equilibrium Vaporization constant evaluated at T and P leaving the j th stage
L	Molar Flow rate of Liquid [kmol/s]
M	Mixture Molecular weight
M^i	Measurement in i phase, where $i = L$ for liquid and V for vapor
M_B, M_D	Holdup in Reboiler, Condenser
\mathbb{N}	Field of all Natural Numbers
N	Molar Transfer rate [kmol/s], or Tray number
n	Stream molar flow rate
n_{McT}	McCabe-Thiele subscript for the Stage n
n_{Sim}	Simulation subscript for the Stage n
P	Pressure, or Probability Function
P_i	Partial Pressure of Component i
Q_B, Q_D	Heat in Reboiler, Condenser
\mathbb{R}	Field of all Real Numbers
R	Gas Constant (8.3145 J/(mol K)), or Reflux Ratio
s	Molar Entropies
T	Temperature
V	Molar Flow rate of Vapor [kmol/s]
v	Molar Volume
x_i	Mole Fraction of component i in the Liquid Phase
x_{Bi}	Mole Fraction in the Bottoms

x_{Di}	Mole Fraction in the Distillate
x_{ji}	Mole Fraction of component i leaving the j th stage
y_i	Mole Fraction of component i in the Vapor Phase
Z	Compressibility Factor

α_{ij}	Relative Volatility of component i with respect to component j for vapor-liquid equilibria
$\gamma(t, \tau)$	Autocovariance
μ	Mean
ρ	Mass Density
$\rho(t, \tau)$	Autocorrelation
σ	Standard Deviation
σ^2	Variance
\forall	for all
\in	Element of
\exists	exists
\subset	Subset of



Abbreviations

AME	Additive Modeling Error
AR	Auto-regressive Process
ARIMA	Auto-regressive, Integrating, Moving Average Model
ARMA	Auto-regressive, Moving Average Process
ARMAX	Auto-regressive, Moving Average Exogenous Model
ARX	Auto-regressive Exogenous Model
DOF	Degrees of Freedom
DAE	Differential Algebraic Equation
ESA	Energy-Separating Agent
EKF	Extended Kalman Filter
FPM	First Principle Model
GC	Gas Chromatography
HMI	Human Machine Interface
LW	Lost Work
MA	Moving Average Process
MME	Multiplicative Modeling Error
MRAC	Model-Reference Adaptive Control
MSA	Mass-Separating Agent
NRTL	Nonrandom, Two-Liquid
ODE	Ordinary Differential Equation
OE	Output-Error Model
PDE	Partial Differential Equation
PID	Proportional-Integral-Derivative
P&ID	Piping and Instrumentation Diagram
SCADA	Supervisory Control And Data Acquisition
SSE	Sum of Squares due to Error
SSR	Sum of Squares due to Regression
TSS	Total Sum of Squares
UKF	Unscented Kalman Filter

Contents

Abstract	i
Resumen	ii
Kurzfassung	iii
Notation	v
Abbreviations	vii
Contents	x
List of Figures	xii
List of Tables	xiii
1 Introduction	1
2 Theoretical Background: Distillation and Distillation Columns	3
2.1 Distillation	3
2.2 Distillation Columns	4
2.3 Binary Distillation	5
2.4 Ponchon-Savarit Method	6
2.5 McCabe-Thiele Method	6
2.5.1 McCabe-Thiele Derivation of Equations	8
2.5.2 McCabe-Thiele Enrichment Lines	10
2.5.3 McCabe-Thiele q -line	12
2.5.4 McCabe-Thiele Overflow	13
2.5.5 McCabe-Thiele Plotting Considerations	13
2.5.6 McCabe-Thiele Effect of Removing Restrictions	14
2.6 Equilibrium Model	15
2.7 Ideal Gas, Ideal Liquid Solution Model	15
2.8 Nonideal Thermodynamic Property Models	17
2.8.1 P - v - T Equation-of-State Models	17
2.8.2 Derived Thermodynamic Properties from P - v - T Models	18
2.9 Liquid Activity-Coefficient Models	20
2.10 Fundamental Principles Involved in Distillation	21
2.10.1 Equilibrium Properties	21

2.10.2	Thermodynamic Properties	22
2.11	Ideal Binary Distillation Column	24
2.12	Nonideal Distillation Column	27
3	Theoretical Background: Modeling a System	29
3.1	Building a Model	29
3.1.1	Time Series Analysis	30
3.1.2	Theoretical Time Series Models	32
3.1.3	Modeling Time Series	34
3.1.4	System Identification Methods	35
3.2	Approximation in Mathematical Model Building	36
3.3	Mathematical Model Types	37
3.4	Model Considerations	37
3.4.1	Regression	37
3.4.2	Design of Experiments	39
3.4.3	Outlier Detection	39
3.4.4	Model Validation	39
3.5	Framework for Physical Modeling	40
4	Mathematical Model of Laboratory-Scale Distillation Column	41
4.1	Laboratory-Scale Distillation Column	41
4.1.1	Laboratory-Scale Distillation Column Process Control System	45
4.2	Laboratory-Scale Distillation Column Structure	46
4.2.1	Variables	48
4.2.2	Condenser	49
4.2.3	Column and Feedpoint	49
4.2.4	Reboiler	50
4.3	Laboratory-Scale Distillation Column Assumptions	51
4.4	Laboratory-Scale Distillation Column Equations	52
4.4.1	Condenser	52
4.4.2	Column and Feed Point	53
4.4.3	Reboiler	54
4.5	Laboratory-Scale Distillation Column Model	55
4.6	Laboratory-Scale Distillation Column Model Simplification	57
5	Simulation of the Laboratory-Scale Distillation Column	59
5.1	Variables	59
5.2	Assumptions for Simulation	60
5.3	Simulation Results	60

6 Comparison of Distillation Column and Nominal Model	63
6.1 Comparison against the McCabe-Thiele method	63
6.2 Comparison against experimental temperatures	68
7 Conclusions and Future Work	72
Appendix	74
Bibliography	78



List of Figures

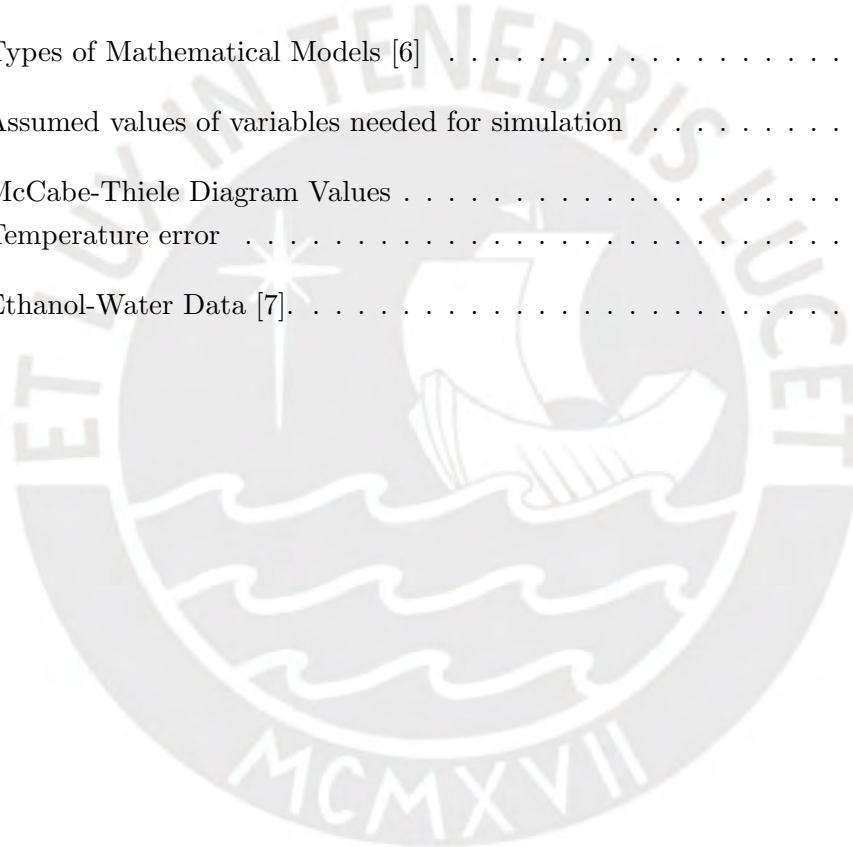
2.1	Schematic Diagram of a Distillation Column [1]	5
2.2	McCabe-Thiele Method [2]	10
2.3	Detailed McCabe-Thiele Method [3]	11
2.4	q -line [2]	12
2.5	Overflow McCabe-Thiele Method [3]	14
2.6	General Separation System	23
4.1	Picture of Ethanol-Water Distillation Plant	41
4.2	Diagram of Ethanol-Water Distillation Plant	42
4.3	Mixing Section and Column of Ethanol-Water Distillation Plant	43
4.4	P&ID of Ethanol-Water Distillation Plant	44
4.5	Hardware structure of the Process Control System	45
4.6	DigiVis - Distillation Plant without Column	46
4.7	DigiVis - Distillation Plant with Column	46
4.8	Column Structure	47
4.9	Diagram of the Condenser	49
4.10	Picture of the Condenser	49
4.11	(a) Diagram of the Column (b) Diagram of a Stage (j)	50
4.12	Picture of the Feed Point	50
4.13	Diagram of the Reboiler	51
4.14	Picture of the Reboiler	51
4.15	Complete diagram of the column	56
5.1	Simulink Model of the Distillation Column	61
5.2	Modeled temperature at each stage	62
5.3	Simulink Model for x_D and y_B	62
5.4	x per stage	62
5.5	y per stage	62
6.1	VLE of Ethanol and Water [4].	63
6.2	α value for different pressures	64

6.3	McCabe-Thiele Diagram for VLE of ethanol-water	65
6.4	McCabe-Thiele Diagram with values for x_j and y_j	65
6.5	Comparison of x per stage between McCabe-Thiele Diagram and Suggested Model	66
6.6	Comparison of y per stage between McCabe-Thiele Diagram and Suggested Model	66
6.7	Concentration Comparison for Stages 1 to 4	67
6.8	Concentration Comparison for Stages 5 to 10	67
6.9	Temperature at each stage	68
6.10	Temperature at each stage after zero-order hold	68
6.11	Compared Temperatures at stage 1 to stage 4	69
6.12	Compared Temperatures at stage 5 to stage 8	70
6.13	Compared Temperatures at Stage 9 and Condenser	70



List of Tables

2.1	Commercial Binary Distillation Operations [5]	6
2.2	Variables used by McCabe and Thiele [3]	8
3.1	Types of Mathematical Models [6]	38
5.1	Assumed values of variables needed for simulation	60
6.1	McCabe-Thiele Diagram Values	64
6.2	Temperature error	71
7.1	Ethanol-Water Data [7]	74



1 Introduction

Distillation processes are widely used in the chemical industry, and as defined in [2], it consists of the separation of miscible liquids with different boiling points. The process consists of boiling the mixed substance and condensing and collecting the vapor. Its applications include producing distilled beverages with a high alcohol content [8], desalination [9], and hydrocarbon industry [10].

Modeling a distillation column will allow us to design adequate controllers using, for example, model-reference adaptive control (**MRAC**). A good model of the distillation column will also allow us to predict how will the system behave under different conditions, and thus, to optimize the system.

Modeling and system identification is an important branch of control engineering. According to Goodwin [11], designing a control system typically requires an interplay between constraints and trade-offs, to find a balance between how fast and accurate it is to reach certain desired value and how much energy is able to be used. To achieve this, it is necessary to understand how a system works, which will be accomplished by finding the mathematical model which describes the steady state and dynamic behavior of a system. The power of a mathematical model lies in the fact that it can be simulated in hypothetical situations, for example, the system's behavior in closed loop or with different parameters, under different disturbances.

Ljung [6] states that two kinds of knowledge can be discerned for model construction. One is the actual knowledge and insights of the process's way of functioning and its properties. The other is the knowledge of how these facts can be transferred into a useful model. He calls these areas of knowledge the domain expert's knowledge (understanding the application and mastering all facts relevant to the model) and the engineer's knowledge (putting the expert's knowledge into practice in a usable and explicit model).

We will focus on mathematical models, this means that the relationships between quantities (flow, current, temperature, *etc*) that can be observed in the system are described as mathematical relationships in the model. There are two sources of knowledge for system properties: the collected experiences of experts and the literature in the area (laws of nature) and the other source is the system itself. The observations of the system and experiments done are the basis for the descriptions of its properties.

The focus of this thesis is concerned with finding the mathematical model of the laboratory-scale distillation column located at the Technical University of Ilmenau.

The main objective is to determine the model of a laboratory-scale ethanol-water distillation column, present in the university, based on **FPM** that will allow concentration on the different stages of the column to be estimated.

Secondary objectives include:

- Investigate system modeling, specifically of distillation processes;
- Develop the theoretical model of the distillation column;
- Simulate and improve the model;
- Compare the model.

2 Theoretical Background: Distillation and Distillation Columns

In this chapter, the theoretical backgrounds of distillation and distillation columns are explained with a main focus on binary distillation and the McCabe-Thiele method.

2.1 Distillation

The creation of a mixture of different materials is a spontaneous process that requires no energy; however, the inverse process requires energy [5]. The most common separation technique is separation by phase addition or creation which requires the creation of a second phase, immiscible with the feed phase, by energy transfer or pressure reduction. A common operation of this type is distillation, which is defined by the *Dictionary of Chemical Engineering* [2] as the physical separation of liquids with different boiling points by boiling the liquid mix and collecting the condensed vapor [12].

In separation by phase addition or creation, if the feed is a single-phase solution then another phase must be added in order to achieve separation of the phases. The second phase is generated either by an energy-separating agent (**ESA**) and/or a mass-separating agent (**MSA**). An **ESA** incorporates heat transfer or transfer of shaft work to or from the mixture [5].

Often, the degree of separation achieved by a single contact of two phases is insufficient because the difference in volatility of the species is not large enough. In that case, multiple stage separation should be considered. In distillation there are multiple contacts between the flowing liquid and vapor. Each contact, called a stage, is often made of horizontal trays arranged in a column. The closer the boiling points of the different liquids are, the more trays the column will need to separate the mixture. When the

volatility difference is too small as to need more than 100 trays, extractive distillation is needed. In this kind of distillation, a miscible **MSA** is needed to act as a solvent [5].

2.2 Distillation Columns

The general distillation plant consists of four parts: distillation column, reboiler, condenser, and feed point.

The *Dictionary of Chemical Engineering* [2] defines a distillation column as a tall vertical cylindrical vessel used for distillation. A distillation column is a space for contacting vapor and liquid stream, by a series of stacked plates (or trays), for the purpose of allowing mass transfer between the two phases. A schematic diagram of a distillation column taken from [1] is shown in Figure 2.1 [13].

In order for the distillation to occur, a liquid feed is introduced in the column onto a feed plate at the feed point, which divides the column into two sections. The section below the feed point of the column is known as the stripping section, in which the less volatile component increase in concentration as the more volatile components are stripped out. While above, it is known as enriching (also called exhausting by McCabe-Thiele) or rectifying section, where the more volatile component in both liquid and vapor increases [2], [5], [1].

Hot vapor rises up the column through perforations in the tray and comes in contact with cooled liquid descending on trays for a long enough period of time for it to reach the vapor-liquid equilibrium. The vapor and liquid phases come into contact because as one molecule of higher boiling material converts from vapor to liquid phase by energy release, another molecule of lower boiling material uses the free energy to convert from liquid to vapor phase. This way, the more volatile component increases in concentration the higher it is in the column [1], [13].

A reboiler (heat exchanger) is then used to boil the bottom product and generate vapor for the column, called boilup. A condenser is used to condense the vapor from the top of the column. A small amount of liquid is returned to the column as reflux [2], [5].

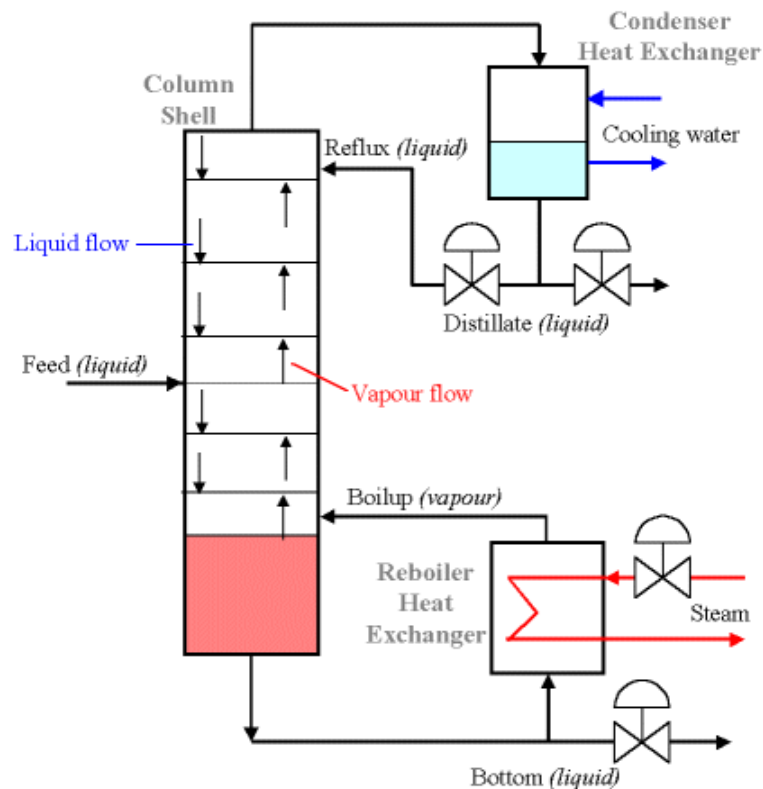


Figure 2.1: Schematic Diagram of a Distillation Column [1]

The products of the distillation column are the distillate (D), liquid or vapor from the top of a distillation process which is rich in the more volatile component, and the bottoms (B) or raffinate, the residual liquid steam leaving from the bottom of the distillation column [2].

2.3 Binary Distillation

Binary distillation is understood as the separation of a two-component mixture. In Table 2.1, taken partially from [5], it is showed a list of common commercial binary distillations in which it is appreciated that both the average relative volatility and the reflux ratio influence the number of trays needed for the separation to occur. The bigger the average relative volatility, the lesser the number of trays needed. And, in the case of the reflux ratio, the higher this is, the less number of theoretical trays that will be needed.

This thesis will focus on ethanol-water distillation. Graphical techniques as Ponchon-Savarit and McCabe-Thiele can determine the separation for continuous binary distillation processes [2].

Binary Mixture	Average Relative Volatility	Number of Trays	Typical Operating Pressure [psia]	Reflux-to-Minimum-Reflux Ratio
Propylene/propane	1.40	138	280	1.06
Methanol/ethanol	1.44	75	15	1.20
Water/acetic acid	1.83	40	15	1.35
Ethylene/ethane	1.87	73	230	1.07
Toluene/ethylbenzene	2.15	28	15	1.20
Propane/1,3-butadiene	2.18	40	120	1.13
Ethanol azeotrope/water	2.21	60	15	1.35
Isopropanol/water	2.23	12	15	1.28
Benzene/toluene	3.09	34	15	1.15
Methanol/water	3.27	60	45	1.31

Table 2.1: Commercial Binary Distillation Operations [5]

2.4 Ponchon-Savarit Method

The Ponchon-Savarit method is a graphical method for the analysis of two heterogeneous liquids by binary distillation. It is used for determining the number of stages needed for a required separation and it is based on a stage-wise approach using enthalpy and composition of each equilibrium stage. This method was developed by M. Ponchon and P. Savarit between 1921 and 1922 [2].

2.5 McCabe-Thiele Method

The McCabe-Thiele method, developed by Warren L. McCabe and Ernest W. Thiele in 1925, is a simpler graphical method for the analysis of two heterogeneous liquids by binary distillation which exhibits its results in a plainer manner than other analytic or graphic methods. For example Sorel's method which involves complicated calculations,

or Lewis-Sorel's method which is the simplification of Sorel's by assuming that the enrichment per plate was small but carried many errors when the number of plates was large. McCabe-Thiele's method is used for determining the number of theoretical plates needed to distill a mixture to the required purity and it is based on stage-wise approach requiring vapor-liquid equilibrium curves of the two liquids [2], [3], [14], [15].

Certain assumptions are made in order to simplify the method. It is shown later that, if necessary, the restrictions can be dismissed without increasing the complexity of the method. The mixture will be separated in product (P) and waste (W) according to McCabe-Thiele nomenclature. The assumptions are the following [3]:

1. The number of moles of vapor ascending the column and the molar overflow is constant from tray to tray;
2. The feed, which is usually preheated by the waste, is introduced into the column at a temperature equal to the boiling point of the liquid on the feed plate;
3. The only condenser is either a simple or a total condenser, and the composition of the product is the same as the one from the vapor in the top plate;
4. The heat is supplied at the base of the column by a heat exchanger, so the condensing steam does not dilute the waste.

Carl Schaschke simplifies this assumptions in [2] to:

1. A constant molar overflow requiring constant molar heats of vaporization;
2. For every liquid mole vaporized, a mole of vapor is condensed;
3. There is no heat of mixing;
4. There is no heat transfer to or from the column.

In order to work with this method, the following rules for nomenclature are taken in consideration [3]:

1. All the concentrations are expressed as mole fractions of the more volatile component;

2. Liquid compositions are denoted by x and vapor compositions by y ;
3. All quantities belonging to the enriching column are distinguished by a line written over them;
4. The plates are numbered from the top plate of the rectifying column to the bottom plate of the enriching column;
5. The feed plate, top plate of the enriching column, will be a plate with a definite number;
6. The subscripts refer to the tray of origin.

Other variables used in this method are shown in the next Table 2.2:

n	General plate in the rectifying column
\bar{n}	General plate in the exhausting column
P	Moles of the distillate withdrawn as product
x_P	Composition of product
F	Moles of the mixture fed to the column
x_F	Composition of feed mixture
W	Moles of waste withdrawn from the column
x_W	Composition of waste
O	Moles overflow from any plate in rectifying column
\bar{O}	Moles overflow from any plate in exhausting column
V	Moles of vapor rising in the rectifying column
\bar{V}	Moles of vapor rising in the exhausting column
A, A', B, B'	coefficients in the enrichment equations

Table 2.2: Variables used by McCabe and Thiele [3]

2.5.1 McCabe-Thiele Derivation of Equations

In an ideal column, by means of balances of total material and more volatile component, Equation 2.1 describes the rectifying column [3].

$$y_{n+1} = \frac{O}{O+1}x_n + \frac{x_p}{O+1} \quad (2.1)$$

This equation can be rewritten as Equation 2.2 which gives way to Equation 2.3, which is called the enrichment equation of the rectifying column or, the rectifying equation [3].

$$A = \frac{O}{O+1},$$

$$B = \frac{x_p}{O+1} \quad (2.2)$$

$$y_{n+1} = Ax_n + B \quad (2.3)$$

Consider the entire section of the column between plates $n+1$ and n , Equation 2.4 shows the material balances in this section [3].

$$\bar{x}_n = \frac{\bar{O} - W}{\bar{O}} \bar{y}_{n+1} + \frac{W}{\bar{O}} x_W \quad (2.4)$$

When assumptions 1 and 2 are made, the heat balance is shown in Equation 2.5 and the material balance for the feed plate is shown in Equation 2.6 and for the entire column it is shown in Equation 2.7 [3].

$$\bar{V} = V \quad (2.5)$$

$$\bar{O} = F + O \quad (2.6)$$

$$F = W + 1 \quad (2.7)$$

Substituting the values for \bar{O} and W from Equations 2.6 and 2.7 into Equation 2.4, results in Equation 2.8. Rewriting this equation using A' and B' as Equation 2.9 gives place to Equation 2.10 which is the equation of a line with a slope of $1/A'$ and an interception with the x -axis in B' . This equation is called the enrichment equation of the exhausting column or the exhausting equation [3].

$$\bar{x}_n = \frac{O+1}{O+F} \bar{y}_{n+1} + \frac{F-1}{O+F} x_W \quad (2.8)$$

$$A' = \frac{O + 1}{O + F},$$

$$B' = \frac{F - 1}{O + F}x_W \quad (2.9)$$

$$\bar{x}_n = A'\bar{y}_{n+1} + B' \quad (2.10)$$

2.5.2 McCabe-Thiele Enrichment Lines

Every binary mixture has a definitive relationship between the composition of the liquid phase (x) and the composition of the vapor phase (y) in equilibrium with it. This relationship is shown better in the form of a rectangular plot of x vs y , with x in the horizontal axis and y in the vertical axis. The curve formed is known as the vapor-liquid equilibrium line, as shown in Figure 2.2 and gives the relationship between x of any tray and of any vapor rising from the same tray [2], [3].

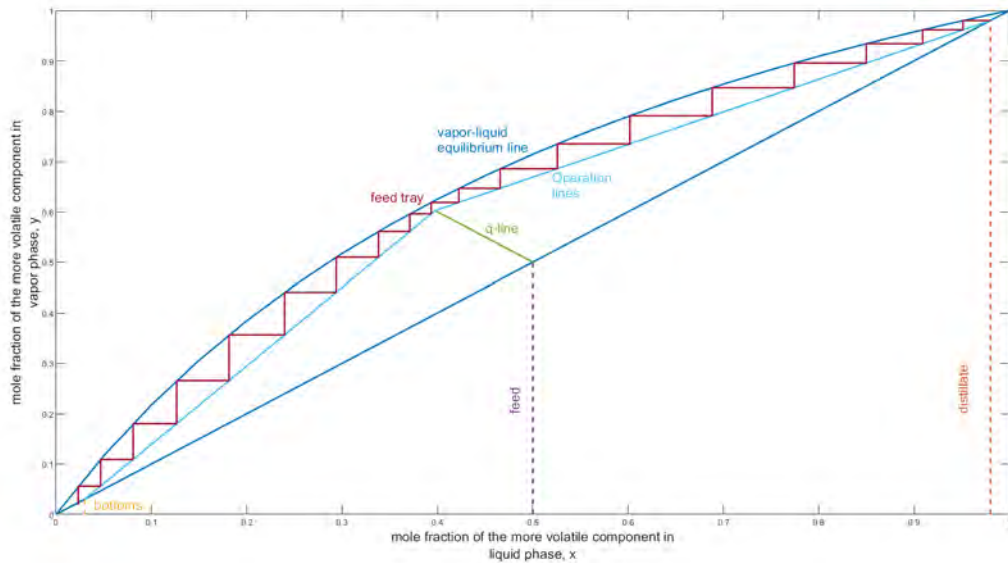


Figure 2.2: McCabe-Thiele Method [2]

The equilibrium curve and Equations 2.3 to 2.10 are sufficient to analytically calculate the compositions of liquid and vapor that belong to each plate, and also the number of theoretical plates needed when the composition of the feed, product and waste, and the magnitudes of the feed and the overflow have been chosen [3].

Once the equilibrium line is plotted, knowing that the condenser used is simple, the concentration of vapor from the top tray (y_1) is the same of the composition of the product (x_P) and, therefore it is known. The value of x_1 can be obtained directly by reading it from the equilibrium line since it is represented by the abscissa of the point on the curve with ordinate y_1 , as shown in Figure 2.3. The coefficients A and B of the Equation 2.3 are calculated from x_P and O . The composition of the vapor rising from plate 2 can be calculated as $y_2 = Ax_1 + B$ and x_2 can be read from the equilibrium line, this value is then used to find y_3 and the same process repeat for each plate. This molar balances over the rectifying and exhausting sections of the column are connected by short horizontal and vertical lines, providing operating lines [3].

The step lines represent the vapor-liquid equilibrium on each equilibrium stage (or theoretical tray) and provide an hint of the number of perfect trays needed for a separation. Analogously, the enrichment from tray to tray in the exhausting section is found by plotting the exhausting line to conform with Equation 2.10 and moving up or down in the same step-wise manner. The interception of the stripping and rectifying sections meets the q -line [2], [3].

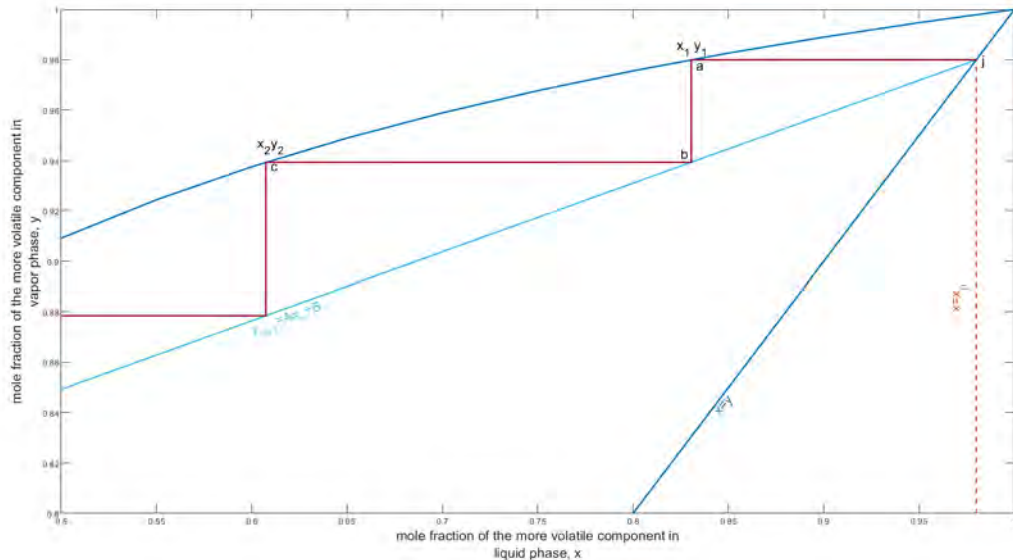


Figure 2.3: Detailed McCabe-Thiele Method [3]

Equations 2.1 and 2.8 show that the orientation of the enrichment lines, line $y_{n+1} = Ax_n + B$ in Figure 2.3, depends only on O for any given values of F , x_P and x_W . If the subscripts are drop from Equation 2.1 and x is set equal to y , O disappears and therefore

y is also equal to x_P showing that the rectifying line crosses the diagonal ($x = y$) at the composition of the product, without the reflux influencing it. Also, if x is equal to zero, then $y = B$ and so, for a definite overflow [3].

The diagonal $x = y$ is also plotted as part of the vapor-liquid equilibrium line for convenience, since the point a in Figure 2.3 is easily located by drawing a vertical line in $x = x_P$, finding its intersection with the diagonal, point j and drawing a horizontal line ja [3].

2.5.3 McCabe-Thiele q -line

The q -line represents the condition of the feed in which q is the mole fraction of the more volatile component of the feed. The slope is $q/(q-1)$ and can be used to indicate the condition of the feed as seen in Figure 2.4. The feed is saturated liquid if $q = 1$ (the q -line is vertical); and saturated vapor if $q = 0$ (the q -line is horizontal) [2], [5].

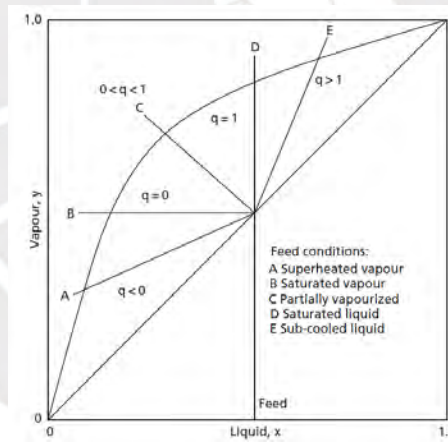


Figure 2.4: q -line [2]

One point of the q -line is the intersection of the rectifying and stripping operation lines. Equation 2.11 describes the rectifying operating line and the Equation 2.12 describes the stripping operation line, rewritten as Equation 2.13; equaling Equations 2.11 to 2.13, we get to the q -line Equation 2.14 [5].

$$y_{n+1} = Ax_n + B \quad (2.11)$$

$$\bar{x}_n = A'\bar{y}_{n+1} + B' \quad (2.12)$$

$$\bar{y}_{n+1} = \frac{1}{A'} \bar{x}_n + \frac{B'}{A'} \quad (2.13)$$

$$y_{n+1} = \frac{q}{q-1} x_n - \frac{x_F}{q-1} \quad (2.14)$$

2.5.4 McCabe-Thiele Overflow

When designing a column, it is important to balance the fixed costs and the heat cost. A theoretical minimum overflow will require an infinite number of plates with an infinite cost of the column, but the cost of the heat is minimum since a minimum quantity of vapor is required to be generated at the bottom of the column; on the other hand, if a infinitely large reflux is assumed, the column will contain a minimum number of perfect plates and the cost of heat will be infinite as a infinite amount of vapor will be needed [3].

By Equations 2.1 and 2.8 it is appreciated that as O increases indefinitely, the slopes of the enrichment lines approach 1, as shown in Equation 2.15 where $N \in \mathbb{N}$ and is a large number [3].

$$y_{n+1} = \lim_{O \rightarrow N} \left(\frac{O}{O+1} x_n + \frac{x_P}{O+1} \right) \quad (2.15)$$

$$y_{n+1} = \frac{x_P + Nx_n}{N+1} \rightarrow \frac{N}{N} = 1$$

For an infinite overflow, as shown in Equation 2.16, the lines coincide with the $x = y$ line and the minimum number of plates is determined by steps, as seen in Figure 2.5. The optimum overflow and the optimum number of plates must be determined by trial [3].

$$y_{n+1} = \lim_{O \rightarrow \infty} \left(\frac{O}{O+1} x_n + \frac{x_P}{O+1} \right) \quad (2.16)$$

$$y_{n+1} = x_n$$

2.5.5 McCabe-Thiele Plotting Considerations

Usually, it is desired for the product to be as pure as possible and for the waste to be exhausted, in terms of the more volatile component; this means that, if plotted in only one diagram, it will be too packed with information at the ends of the equilibrium curve

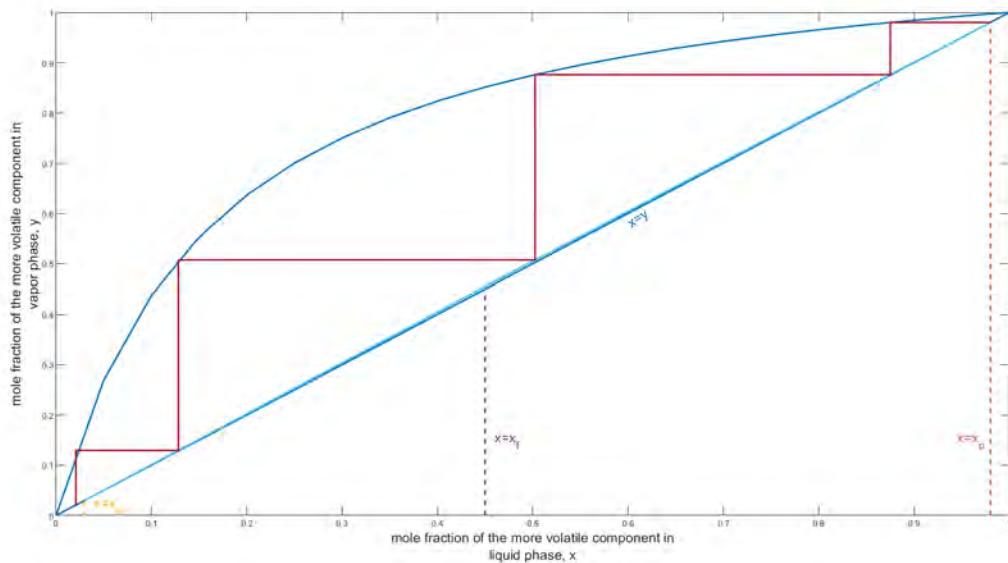


Figure 2.5: Overflow McCabe-Thiele Method [3]

too use it with precision. Therefore, separate, enlarged diagrams of these two sections must be made. The equilibrium curve will follow Raoult's law¹ at the top and Henry's law² at the bottom [3].

2.5.6 McCabe-Thiele Effect of Removing Restrictions

In this subsection, the effect of removing the initial two of the four initial assumptions will be considered. The effect of the feed not being a wholly liquid at its boiling point and the effect of variation on molar overflow will not be considered in the scope of this thesis.

If a partial condenser is used instead of a total condenser, then the vapor that rises from the top plate is weaker than the product; as long as the composition of the product is known, the enrichment equation is not affected. The beginning step will be $y = y_1$ instead of $y = x_P$ [3].

¹Raoult's Law: The partial pressure (P_A) exerted by each component (A) in an ideal liquid mixture is the product of the vapor pressure (p_A) of each component and its mole fraction (x_A) at the temperature of the liquid, expressed as $P_A = x_A p_A$ [2].

²Henry's Law: Describes the relationship between the concentration of a gas dissolved in a liquid at the equilibrium partial pressure and constant temperature, expressed as $P_A = H x_A$, where P_A is the partial pressure of component A and H is Henry's constant [2].

When using open steam, the waste is diluted by this steam. The latent heat of condensation of the incoming steam will vaporize an equal weight of mixture and the moles of steam used will be equal to the moles of vapor sent up the column (\bar{V}) which is equal to $O+1$. If W' is the number of moles of diluted waste and x'_W its composition, then $Wx_W = W'x_{W'}$. Therefore, it is necessary to take the steps to the x -axis to allow for the effect of open steam [3].

2.6 Equilibrium Model

The equilibrium model, based on the assumption that tray in the column is considered a theoretical tray (equilibrium plate) at a specified P and T , means that the vapor and liquid leave the tray in a thermodynamic equilibrium. A phase-equilibrium ratio is the ratio of mole fractions of a species in two different phases at equilibrium. For vapor-liquid systems, the constant is referred to as the vapor-liquid equilibrium ratio (K - value) defined by Equation 2.17 [5].

$$K_i \equiv \frac{y_i}{x_i} \quad (2.17)$$

For the equilibrium-stage calculations, separation factors are defined by forming ratios of equilibrium ratios. For the vapor-liquid case, the relative volatility (α_{ij}) is defined by Equation 2.18, separations will be easier for very large values of (α_{ij}) [5].

$$\alpha_{ij} \equiv \frac{K_i}{K_j} \quad (2.18)$$

2.7 Ideal Gas, Ideal Liquid Solution Model

The simplest model is given when both liquid and vapor phases are ideal solutions and the vapor is an ideal gas, then the classic thermodynamics relationships of P - v - T , also known as equation-of-state models are met at pressures up to 345 kPa [5].

The molar volume (v) and the mass density (ρ) for the vapor are calculated with Equation 2.19, which requires a mixture molecular weight (M) and the gas constant (R),

it assumes that both Dalton's law of additive partial pressures (the total pressure of an ideal mixture of gases and vapors is equal to the sum of the partial pressures of its components) and Amagat's law³ of additive volumes (the total volume of an ideal gas is equal to the sum of the pure component volumes) apply [2], [5].

$$v_V = \frac{V}{\sum_{i=1}^C N_i} = \frac{M}{\rho_V} = \frac{RT}{P}, \quad (2.19)$$

$$M = \sum_{i=1}^C y_i M_i$$

The vapor enthalpy (h_V) is calculated from Equation 2.20 by integrating an equation in temperature from zero-pressure heat capacity at constant pressure ($C_{P_v}^0$) from a reference temperature (T_0) to the temperature of interest and then adding the resulting species vapor enthalpies on a mole-fraction basis [5].

$$h_v = \sum_{i=1}^C y_i \int_{T_0}^T (C_{P_v}^0)_{iV} dT = \sum_{i=1}^C y_i h_{iV}^0 \quad (2.20)$$

The vapor entropy (s_V) is calculated from Equation 2.21 by integrating ($C_{P_v}^0/T$) from (T_0) to (T) for each species, summing on a mole-fraction basis where the first term is (s_V^0). The liquid molar volume and mass density are computed for the pure species using Equation 2.22 and assuming additive volumes [5].

$$s_v = \sum_{i=1}^C y_i \int_{T_0}^T \frac{(C_{P_v}^0)_{iV}}{T} dT - R \ln \left(\frac{P}{P_0} \right) - R \sum_{i=1}^C y_i \ln y_i \quad (2.21)$$

$$v_L = \frac{V}{\sum_{i=1}^C N_i} = \frac{M}{\rho_L} = \sum_{i=1}^C x_i v_{iL}, \quad (2.22)$$

$$M = \sum_{i=1}^C x_i M_i$$

The enthalpy of an ideal-liquid mixture is calculated by subtracting the enthalpy of vaporization from the ideal vapor enthalpy for each species as shown in Equation 2.23. The entropy is obtained in a similar manner as shown in Equation 2.24. Finally, the ideal K -value where the assumption of Dalton's law give the Raoult's law K -value in Equation 2.25 [5].

$$h_L = \sum_{i=1}^C x_i (h_{iV}^0 - \Delta H_i^{vap}) \quad (2.23)$$

³For an ideal gas, the total volume occupied by a mixture is equal to the sum of the pure component volumes: $V = V_A + V_B + \dots$ [2].

$$s_L = \sum_{i=1}^C x_i \left[\int_{T_0}^T \frac{(C_P^0)_{iv}}{T} dT - \frac{\Delta H_i^{vap}}{T} \right] - R \ln \left(\frac{P}{P_0} \right) - R \sum_{i=1}^C x_i \ln x_i \quad (2.24)$$

$$K_i = \frac{P_i^s}{P} \quad (2.25)$$

The ideal K -value is independent of compositions, but exponentially dependent on temperature and inversely proportional to pressure [5].

2.8 Nonideal Thermodynamic Property Models

There are two types of models: P - v - T equation-of-state models and free-energy models; their applicability depends on the components of the mixture and the reliability of the equation constants [5].

2.8.1 P - v - T Equation-of-State Models

The simplest is the ideal gas law, seen in the previous section, which applies only at low pressures or high temperatures. This model neglects the volume occupied by the molecules and the inter-molecular forces, all other equations of state attempt to correct these deficiencies. Based on the ideal-gas law from Equation 2.26 and the van der Waals Equation 2.27 where a and b are species-dependent constants, the law of corresponding states Z is derived in Equation 2.28, also known as generalized equations of state [5].

$$P = \frac{RT}{v} \quad (2.26)$$

$$P = \frac{RT}{v-b} - \frac{a}{v^2} \quad (2.27)$$

$$P = \frac{ZRT}{v}, \quad (2.28)$$

$$Z = Z\{P_r, T - r, Z_{cor}\omega\}$$

Redlich and Kwong proposed an equation of states, the R-K Equation 2.29, with two constants that can be determined from T_c and P_c by applying the critical conditions. Soave added a third factor, the acentric factor ω to the R-K Equation resulting in the S-R-K Equation 2.30 which was accepted for applications to hydrocarbon mixtures because

of its accuracy. Peg and Robinson modified the R-K and S-R-K equations to achieve improved agreement in the critical region and for liquid molar volume with state Equation P-R 2.31, this equation is widely used in calculations for saturated vapors and liquids [5].

$$P = \frac{RT}{v-b} - \frac{a}{v^2 + bv} \quad (2.29)$$

$$b = \frac{0.08664RT_c}{P_c}$$

$$a = \frac{0.42748R^2T_c^{2.5}}{P_cT^{0.5}}$$

$$P = \frac{RT}{v-b} - \frac{a}{v^2 + bv} \quad (2.30)$$

$$b = \frac{0.08664RT_c}{P_c}$$

$$a = \frac{0.42748R^2T_c^2[1 + f_\omega(1 - T_r^{0.5})]^2}{P_c}$$

$$f_\omega = 0.48 + 1.574\omega - 0.176\omega^2$$

$$P = \frac{RT}{v-b} - \frac{a}{v^2 + 2bv - b^2} \quad (2.31)$$

$$b = \frac{0.07780RT_c}{P_c}$$

$$a = \frac{0.45724R^2T_c^2[1 + f_\omega(1 - T_r^{0.5})]^2}{P_c}$$

$$f_\omega = 0.37464 + 1.54226\omega - 0.26992\omega^2$$

2.8.2 Derived Thermodynamic Properties from P - v - T Models

If a temperature-dependent, ideal-gas heat capacity Equation 2.32 or enthalpy Equation 2.38 is available, all vapor- and liquid-phase properties can be derived. The mixture enthalpy Equation 2.34, the mixture entropy Equation 2.35, the pure-component fugacity coefficient Equation 2.36 and the partial fugacity coefficient Equation 2.37 are as follows [5].

$$C_{P_V}^0 = [a_0 + a_1T + a_2T^2 + a_3T^3 + a_4T^4]R \quad (2.32)$$

$$h_V^0 = \int_{T_0}^T C_{P_V}^0 dT = \sum_{K=1}^5 \frac{a_{k-1}(T^k - T_0^k)R}{k} \quad (2.33)$$

$$(h - h_V^0) = Pv - RT - \int_{\infty}^v \left[P - T \left(\frac{\partial P}{\partial T} \right)_v \right] dv \quad (2.34)$$

$$(s - s_V^0) = \int_{\infty}^v \left(\frac{\partial P}{\partial T} \right)_v dv - \int_{\infty}^v \frac{R}{v} dv \quad (2.35)$$

$$\phi_{iV} = \exp \left[\frac{1}{RT} \int_0^P \left(v - \frac{RT}{P} \right) dP \right] = \exp \left[\frac{1}{RT} \int_v^{\infty} \left(P - \frac{RT}{v} \right) dv - \ln Z + (Z - 1) \right] \quad (2.36)$$

$$\bar{\phi}_{iV} = \left\{ \frac{1}{RT} \int_V^{\infty} \left[\left(\frac{\partial P}{\partial N_i} \right)_{T,V,N_j} - \frac{RT}{V} \right] dV - \ln Z \right\} \quad (2.37)$$

$$V = v \sum_{i=1}^C N_i$$

For ideal gases, the ideal gas law from Equation 2.26 is substituted into Equations 2.34 to 2.37 and the results for vapor are $(h - h_V^0) = 0$, $\phi = 1$ for the enthalpy and $(s - s_V^0) = 0$, $\phi = 1$ for the entropy. On the other hand, when the R-K Equation 2.29 is substituted into these equations, the results for vapor are show as Equations 2.38 to 2.41 [5].

$$h_V = \sum_{i=1}^C (y_i h_{iV}^0) + RT \left[Z_V - 1 - \frac{3A}{2B} \ln \left(1 + \frac{B}{Z_V} \right) \right] \quad (2.38)$$

$$s_V = \sum_{i=1}^C (y_i s_{iV}^0) - R \ln \left(\frac{P}{P_0} \right) - R \sum_{i=1}^C (y_i \ln y_i) + R \ln(Z_V - B) \quad (2.39)$$

$$\phi_V = \exp \left[Z_V - 1 - \ln(Z_V - B) - \frac{A}{B} \ln \left(1 + \frac{B}{Z_V} \right) \right] \quad (2.40)$$

$$\bar{\phi}_{iV} = \exp \left[(Z_V - 1) \frac{B_i}{B} - \ln(Z_V - B) - \frac{A}{B} \left(2\sqrt{\frac{A_i}{A}} - \frac{B_i}{B} \right) \ln \left(1 + \frac{B}{Z_V} \right) \right] \quad (2.41)$$

The results of the liquid phase are identical if y_i and Z_V are replaced by x_i and Z_L , the liquid phase forms of Equations 2.38 and 2.39 represent the enthalpy and entropy of vaporization. The liquid enthalpy is determined by accounting for four effects (vapor at zero pressure, pressure correction for vapor to saturation pressure, latent heat of vaporization, and correction to liquid for pressure in excess saturation pressure) at a temperature below the critical [5].

2.9 Liquid Activity-Coefficient Models

If the mixture is an aqueous solution with no polar organic compounds, the model used should be the nonrandom, two-liquid model (NRTL). This model, widely used for vapor-liquid systems, correlates the activity coefficients (γ_i) of a compound with its mole fractions (x_i). The general equation is given by Equation 2.42 where G_{ji} is given by Equation 2.43 and τ coefficients are given by Equations 2.44 and 2.45 where the g values are energies of interaction for molecule pairs. The parameter α_{ji} describes the tendency of species j and i to be nonrandomly distributed with values between 0.2 and 0.47, it is considered $\alpha_{ji} = 0.3$ for nonpolar compounds of ethanol/water [5].

$$\ln \gamma_i = \frac{\sum_{j=1}^C \tau_{ji} G_{ji} x_j}{\sum_{k=1}^C G_{ki} x_k} + \sum_{j=1}^C \left[\frac{x_j G_{ij}}{\sum_{k=1}^C G_{kj} x_k} \left(\tau_{ij} - \frac{\sum_{k=1}^C x_k \tau_{kj} G_{kj}}{\sum_{k=1}^C G_{kj} x_k} \right) \right] \quad (2.42)$$

$$G_{ji} = \exp(-\alpha_{ji} \tau_{ji}) \quad (2.43)$$

$$\tau_{ij} = \frac{g_{ij} - g_{jj}}{RT} \quad (2.44)$$

$$\tau_{ji} = \frac{g_{ji} - g_{ii}}{RT} \quad (2.45)$$

For a binary mixture, the following equations are used [16]:

$$\ln \gamma_1 = x_2^2 \left[\tau_{21} \left(\frac{G_{21}}{x_1 + x_2 G_{21}} \right)^2 + \frac{\tau_{12} G_{12}}{(x_2 + x_1 G_{12})^2} \right], \quad (2.46)$$

$$\ln \gamma_2 = x_1^2 \left[\tau_{12} \left(\frac{G_{12}}{x_2 + x_1 G_{12}} \right)^2 + \frac{\tau_{21} G_{21}}{(x_1 + x_2 G_{21})^2} \right], \quad (2.47)$$

$$\ln G_{12} = -\alpha_{12} \tau_{12},$$

$$\ln G_{21} = -\alpha_{21} \tau_{21},$$

$$\tau_{12} = \frac{\Delta g_{12}}{RT} = \frac{U_{12} - U_{22}}{RT},$$

$$\tau_{21} = \frac{\Delta g_{21}}{RT} = \frac{U_{21} - U_{11}}{RT},$$

where R is the gas constant, T the absolute temperature, U_{ij} the energy between the molecular surface i and j , and U_{ii} the energy of evaporation [16].

2.10 Fundamental Principles Involved in Distillation

For any stage in equilibrium, it is important to assume the following [5]:

1. Each stage achieves phase equilibrium;
2. No chemical reactions happen in a stage;
3. Liquid droplets in vapor are negligible;
4. Vapor bubbles in liquid are negligible.

In order to calculate the composition of the distillate (D) and the bottoms (B), it is necessary to obtain a solution to the following equations, known as the MESH equations [5], [13].

1. **M**aterial balance for each component
2. **E**quilibrium relation for each component
3. **S**ummary of mole-fraction summations for each stage
4. **H** equation: energy balance for each stage

2.10.1 Equilibrium Properties

A mixture of two phases is said to be in physical equilibrium if the following conditions are satisfied [13]:

1. The temperature of the vapor phase (T^V) is equal to the temperature of the liquid phase (T^L);
2. The total pressure in the vapor phase (P^V) is equal to the total pressure in the liquid phase (P^L);

3. The propensity of each component to change from liquid phase to vapor phase is the same as from vapor phase to liquid phase.

Therefore, the temperature of the stage will be $T = T^V = T^L$ and the pressure $P = P^V = P^L$ and Raoult's law $P y_i = P_i x_i$ is also considered. The separation of a binary mixture may be presented in a two-dimensional space. The equilibrium relationships and the material balances equations required to describe an distillation column are Equation 2.48 and Equation 2.49 respectively [13].

$$\text{Equilibrium relationships} \begin{cases} y_{ji} = K_{ji} x_{ji} & (i = 1, 2) \\ & (j = 1, 2, \dots, N) \\ \sum_{i=1}^2 y_{ji} = 1 & (j = 1, 2, \dots, N) \\ \sum_{i=1}^2 x_{ji} = 1 & (j = 1, 2, \dots, N) \end{cases} \quad (2.48)$$

$$\text{Material balances} \begin{cases} V_r y_{j+1,i} = L_r x_{ji} + D X_{Di} & (i = 1, 2) \\ & (j = 1, 2, \dots, f - 1) \\ V_s y_{j+1,i} = L_s x_{ji} - B x_{Bi} & (i = 1, 2) \\ & (j = f, f + 1, \dots, N - 1) \\ F X_i = D X_{Di} + B x_{Bi} & (i = 1, 2) \end{cases} \quad (2.49)$$

2.10.2 Thermodynamic Properties

In Figure 2.6 it is represented a continuous, steady-state, flow chart for a general separation system inspired on [5], where the Heat transfer in and out are denoted by Q_{in} and Q_{out} respectively; and shaft Work denoted by W_s . For each stream, the following variables are considered: Stream molar flow rate (n), Component mole fractions (z_i), Temperature (T), Pressure (P), Molar enthalpies (h), Molar entropies (s), Molar availabilities (b) and Molar Volume (v) [5].

At steady state, if kinetic, potential and surface energy changes are neglected, the First Law of Thermodynamics equation 2.50 refers to the energy balance; while the Second Law of Thermodynamics equation 2.51 refers to the entropy balance [5].

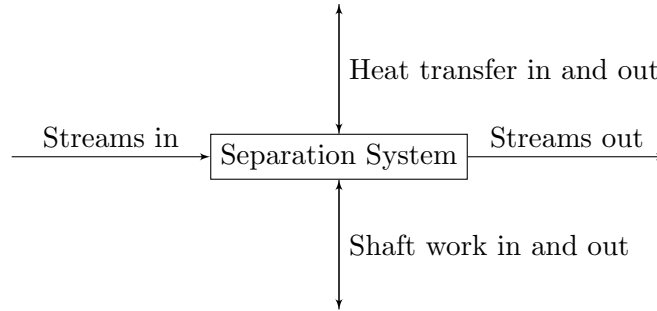


Figure 2.6: General Separation System

$$\sum_{outofsystem} (nh + Q + W_s) - \sum_{intosystem} (nh + Q + W_s) = 0 \quad (2.50)$$

$$\sum_{outofsystem} \left(ns + \frac{Q}{T_s} \right) - \sum_{intosystem} \left(ns + \frac{Q}{T_s} \right) = \Delta S_{irr} \quad (2.51)$$

Since Equation 2.51 predicts the generation of entropy, ΔS_{irr} which is the irreversible increase in entropy of the universe. A more convenient measure of process inefficiency is lost work (LW) defined by Equation 2.52. It is referred as the availability balance where availability means available for complete conversion to shaft work. The availability function b is defined by Equation 2.53 and it is a measure of the maximum amount of energy converted to shaft work if the stream is taken to the reference state. Availability, like entropy, is not conserved in an irreversible process, the difference is LW represented by Equation 2.54 which is always positive [5].

$$LW = \sum_{intosystem} \left[\left(nb + Q \left(1 - \frac{T_0}{T_s} \right) + W_s \right) \right] - \sum_{outofsystem} \left[\left(nb + Q \left(1 - \frac{T_0}{T_s} \right) + W_s \right) \right] \quad (2.52)$$

$$b = h - T_0 s \quad (2.53)$$

$$LW = T_0 \Delta S_{irr} \quad (2.54)$$

It is important to note that the vapor and liquid phases on a given tray approach thermal, pressure and composition equilibrium depending on the efficiency of the plate [1].

2.11 Ideal Binary Distillation Column

It is assumed to have a binary system with constant relative volatility along the column and theoretical trays. This means that the vapor-liquid equilibrium relationship can be written as Equation 2.55 where α is the relative volatility, x_n is the mole fraction of the more volatile component in liquid composition of the n th tray and, analogously, y_n is the vapor composition [17].

$$y_n = \frac{\alpha x_n}{1 + (\alpha - 1)x_n} \quad (2.55)$$

The overhead vapor is totally condensed and flows into the reflux receptacle, with a holdup of liquid M_D (mol). The content of the receptacle is assumed to be perfectly mixed and with x_D composition and at its bubble point⁴. The reflux is pumped back to the top tray (N_T) at a rate R , the overhead distillate product is removed at rate D . The dead time in both the vapor line from the top of the column to the reflux drum and in the reflux line back to the top tray is neglected (this is not the case for small-scale laboratory columns). Its feed is introduced as a saturated liquid onto the feed tray N with a flow rate of F in (mol/min) and a composition z expressed as a mole fraction of the more volatile component. Liquid bottom product is removed at a rate B with a composition x_B . Vapor boilup is generated in a reboiler at rate V . The content of the reboiler is assumed to be perfectly mixed with x_B composition and total holdup M_B (mol). The column contains N_T trays and each tray has a liquid holdup of M_n [17].

Assuming also that there exists an equimolal overflow, whenever a mole of vapor condenses, it vaporizes a mole of liquid. Heat losses and temperature changes from tray to tray are negligible. This means that the vapor and liquid rates in both the stripping and rectifying sections will be constant under steady state conditions [17].

The assumptions above, mean that the vapor rate through all trays is the same, e.g: $V = V_1 = V_2 = \dots = V_{N_T}$. The effect of assuming equimolal overflow is that only one energy equation will be required. The liquid rates along the column will not be the same; therefore, detailed tray hydraulic equations that include the effects of vapor rate, densities, compositions, *etc* should be considered. It is assumed a functional relationship between liquid holdup and liquid rate as Equation 2.56 [17].

⁴Temperature at which bubbles of vapor first appear [2].

$$M_n = f(L_n) \quad (2.56)$$

In commercial scale columns, the response from the heat exchangers (condenser and reboiler) is much faster than the column itself, hence, the dynamics of these exchanger is neglected. With all these assumptions, the behavior of the system can be represented as follows from Equations 2.57 to 2.70 [17].

For the condenser and reflux drum:

Total continuity:

$$\frac{dM_D}{dt} = V - R - D \quad (2.57)$$

Component continuity:

$$\frac{d(M_D x_D)}{dt} = V y_{N_T} - (R + D) x_D \quad (2.58)$$

For the Top tray ($n = N_T$):

Total continuity:

$$\frac{dM_{N_T}}{dt} = R - L_{N_T} \quad (2.59)$$

Component continuity:

$$\frac{d(M_{N_T} x_{N_T})}{dt} = R x_D - L_{N_T} x_{N_T} + V y_{N_T-1} - V y_{N_T} \quad (2.60)$$

For the next top tray ($n = N_T - 1$):

Total continuity:

$$\frac{dM_{N_T-1}}{dt} = L_{N_T} - L_{N_T-1} \quad (2.61)$$

Component continuity:

$$\frac{d(M_{N_T-1} x_{N_T-1})}{dt} = L_{N_T} x_{N_T} - L_{N_T-1} x_{N_T-1} + V y_{N_T-2} - V y_{N_T-1} \quad (2.62)$$

For the n th tray:

Total continuity:

$$\frac{dM_n}{dt} = L_{n+1} - L_n \quad (2.63)$$

Component continuity:

$$\frac{d(M_n x_n)}{dt} = L_{n+1} x_{n+1} - L_n x_n - V y_{n-1} - V y_n \quad (2.64)$$

For the feed tray ($n = N_F$):

Total continuity:

$$\frac{dM_{N_F}}{dt} = L_{N_F+1} - L_{N_F} + F \quad (2.65)$$

Component continuity:

$$\frac{d(M_{N_F} x_{N_F})}{dt} = L_{N_F+1} x_{N_F+1} - L_{N_F} x_{N_F} + V y_{N_F-1} - V y_{N_F} + Fz \quad (2.66)$$

For the first tray ($n = 1$):

Total continuity:

$$\frac{dM_1}{dt} = L_2 - L_1 \quad (2.67)$$

Component continuity:

$$\frac{d(M_1 x_1)}{dt} = L_2 x_2 - L_1 x_1 + V y_B - V y_1 \quad (2.68)$$

For the reboiler and column base:

Total continuity:

$$\frac{dM_B}{dt} = L_1 - V - B \quad (2.69)$$

Component continuity:

$$\frac{dM_B x_B}{dt} = L_1 x_1 - V y_B - Bx \quad (2.70)$$

2.12 Nonideal Distillation Column

In order to calculate the equations for nonideal columns, the following assumptions are made by Luyben [17]:

1. Nonideal conditions:
 - a) Nonideal column components
 - b) Nonequimodal overflow
 - c) Inefficient trays
2. Liquid on trays is completely mixed and incompressible
3. Tray vapor holdups are negligible
4. Dynamics of condenser and reboiler are neglected
5. Vapor and liquid are in thermal equilibrium but not in phase equilibrium

Murphree plate efficiency, which measures the closeness to equilibrium on a plate, is used to describe the departure from equilibrium. For binary distillation, it is presented as Equation 2.71, where n and $n - 1$ refer to the outlet and inlet vapor streams to a stage and y^* is the equilibrium vapor concentration [2], [17].

$$\eta = \frac{y_n - Y_{n-1}}{y^* - y_{n-1}} \quad (2.71)$$

It is important to note that after a grade of purity, depending on the process, the mixture becomes an azeotrope⁵ and further separation by conventional distillation cannot be made [18], [19].

⁵Mixture of two liquids that boils at a constant composition, that is: composition of the vapor is the same as the composition of the liquid. Azeotropes occur due to deviation of Raoult's law, which can be positive or negative [2].

3 Theoretical Background: Modeling a System

There are two basic principles for model construction [6]:

1. Physical Modeling, also called a first principle model (**FPM**): Break down the properties of the system to subsystems whose behaviors are previously known.
2. System Identification as black-box: Use observation from the system in order to fit the model's properties to those of the system.

This thesis focus is the physical model; however, a small peak into system identification will be shown in the subsection 3.1.4. A suitable nominal model should contain all the control relevant features of the plant dynamics and its nonlinearities, it is assumed to be usable for an adequate representation and to be able of being described as analytic data¹. The main objective of analytic modeling is to accomplish finding a function:

$$f : B \subset \mathbb{R}^n \rightarrow \mathbb{R},$$

where the domain B is a subset of \mathbb{R}^n ; depending on the dimension of n , models can be categorized as uni-variate models ($n = 1$) and multivariate models ($n \geq 2$) [20].

3.1 Building a Model

The nominal plant model is the usually the basis for control design, yet it is the real plant that will be controlled by the controller. One of the goals of system modeling is to enable the design of a controller that when controlling the true plant, continues to perform as expected. If this is the case, the controller will be called robust. To achieve this, it is often needed to have a measure of the modeling error, so that convenient pre-

¹Functions or mappings of one or more variables [20].

cautions will be considered in the design stage [11], [21].

There are examples where highly detailed physical models were found but they had limited value for the control system design, either because they had so many free parameters that it was impossible to calibrate them for the real process or because they missed to describe important properties which were ultimately found to dominate controller performance [11], [20].

To build an adequate model, the relevant process variables must be defined and also have into account that there are phenomenological laws which regulate the behavior of the signals in the system. These laws are inherent to the nature of the system and include physical or chemical properties. Phenomenological observations are crucial to understanding the system's dynamics, nonlinearities and important time variations. Process models include both, interdependence on the accumulated (integrated) effect of process variables and dependencies on the sensitivity to change (differential) of variables [11].

The data necessary for the model is considered to be a time series². For the analysis of a time series, three different approaches are evaluated [22]:

1. **Transfer function-based approach:** Describes the observable system with the information available. The system's internal dynamics are not considered.
2. **State-space-based approach:** Describes the internal process dynamics. Incorporates the Kalman filter³ for appropriate parameter estimates.
3. **Frequency-domain-based approach:** Describes the process in the frequency domain. Usually needs a Fourier transformation of the data set.

3.1.1 Time Series Analysis

Statistical properties (mean or standard deviation) may depend on time. Therefore, assumptions are made about the the time series. It is called strictly stationary if the

²Data set where the time element is important [22].

³The Kalman filter, developed by Kalman [23], combines the prediction of the estimate with the update estimate growing a memory filter for online improving of the estimate and its covariance. The extended Kalman filter (**EKF**) and the unscented Kalman filter (**UKF**) are some of the variations for nonlinear parameter estimation [24], [25], [26].

probabilistic behavior P of every subset is identical to the one of the time shifted set, as shown in Equation 3.1 where j are the number of samples, t are the time points and k are the shifts. It is sometimes complicated to determine if a data set satisfies this condition. Hence, a time series will be weakly stationary if it complies with the next three statements [22].

1. It has a finite variance.
2. Its mean is constant and independent of time, as shown in Equation 3.2.
3. The autocovariance function, Equation 3.3 where t is the time and τ is the lag, is independent of time.
4. (or, instead of 3.) The autocorrelation, Equation 3.4, is independent of time.

$$P(x_t, x_{t+1}, \dots, x_{t+j}) = P(x_{t+k}, x_{t+1+k}, \dots, x_{t+j+k}) \quad (3.1)$$

$$\mu = E(x_t) \quad (3.2)$$

$$\gamma(t, \tau) = E\left((y_t - E(y_t))(y_{t+\tau} - E(y_{t+\tau}))^T\right) \quad (3.3)$$

$$\rho(t, \tau) = \frac{\gamma(t, \tau)}{\gamma(t, 0)} = \frac{\gamma(t, \tau)}{\sigma_t^2} \quad (3.4)$$

Since both the autocovariance and the autocorrelation do not depend on t , the Equations 3.3 and 3.4 can be rewritten as Equations 3.5 and 3.6 respectively, where μ_Y is the mean value of the time series.

$$\gamma(\tau) = E\left((y_t - \mu_Y)(y_{t+\tau} - \mu_Y)^T\right) \quad (3.5)$$

$$\rho(\tau) = \frac{\gamma(\tau)}{\gamma(0)} = \frac{\gamma(\tau)}{\sigma_y^2} \quad (3.6)$$

3.1.2 Theoretical Time Series Models

Some time series models will be examined in this subsection.

Process: White Noise

A white noise signal is defined by Equation 3.7, where $e_t \sim \mathfrak{N}(0, \sigma^2)$. The mean of the signal is represented as Equation 3.8 and the autocovariance, by Equation 3.9. Its autocorrelation is a single peak at $\tau = 0$ [22].

$$y_t = e_t \quad (3.7)$$

$$\mu_y = E(y_t) = E(e_t) = 0 \quad (3.8)$$

$$\gamma_y(\tau) = E(y_t y_{t-\tau}) = E(e_t e_{t-\tau}) = \begin{cases} \sigma^2, & \tau = 0 \\ 0 & \text{otherwise} \end{cases} \quad (3.9)$$

Process: Moving Average

A moving average process, $\mathbf{MA}(q)$, is defined by Equation 3.10, where $e_t \sim \mathfrak{N}(0, \sigma^2)$. The mean value is zero. The autocovariance is represented by Equation 3.11, its variance is represented by Equation 3.12 and its autocorrelation is represented by Equation 3.13 showing q significant peaks [22].

$$y_t = e_t + \beta_1 e_{t-1} + \beta_2 e_{t-2} + \dots + \beta_q e_{t-q} = \sum_{i=0}^q \beta_i e_{t-i} \quad (3.10)$$

$$\gamma(\tau) = \begin{cases} \sum_{i=0}^{q-\tau} \beta_i \beta_{i+\tau} \sigma^2 & \tau \leq q \\ 0 & \text{otherwise} \end{cases} \quad (3.11)$$

$$\gamma(0) = \sum_{i=0}^q \beta_i^2 \sigma^2 \quad (3.12)$$

$$\rho(\tau) = \begin{cases} \frac{\sum_{i=0}^{q-\tau} \beta_i \beta_{i+\tau}}{\sum_{i=0}^q \beta_i^2} & \tau \leq q \\ 0 & \text{otherwise} \end{cases} \quad (3.13)$$

Process: Autoregressive

An autoregressive process, $\mathbf{AR}(p)$, is defined by Equation 3.14, where $e_t \sim \mathcal{N}(0, \sigma^2)$. The mean value is represented by Equation 3.15, where the coefficients h_i can be obtained by dividing the polynomial from Equation 3.14. The autocovariance is represented by Equation 3.16, its variance is represented by Equation 3.17 and its autocorrelation is represented by Equation 3.18 showing an exponential decay [22].

$$y_t = e_t - \alpha_1 y_{t-1} - \alpha_2 y_{t-2} - \dots - \alpha_p e_{t-p} = e_t - \sum_{i=0}^p \alpha_i y_{t-i} \quad (3.14)$$

$$= \frac{1}{1 + \alpha_1 z^{-1} + \alpha_2 z^{-2} + \dots + \alpha_p z^{-p}} e_t$$

$$\mu_y = E(y_t) = \sum_{i=0}^{\infty} h_i E(e_{t-i}) = 0 \quad (3.15)$$

$$\gamma(\tau) = \sum_{i=1}^p \sum_{j=1}^p \frac{(-\theta_j)^\tau \phi_i \phi_j}{1 - \theta_i \theta_j} \sigma^2 \quad (3.16)$$

$$\sigma_y^2 = \gamma(0) = \sum_{i=1}^p \sum_{j=1}^p \frac{\phi_i \phi_j}{1 - \theta_i \theta_j} \sigma^2 \quad (3.17)$$

$$\rho(\tau) = \frac{\sum_{i=1}^p \sum_{j=1}^p \frac{(-\theta_j)^\tau \phi_i \phi_j}{1 - \theta_i \theta_j}}{\sum_{i=1}^p \sum_{j=1}^p \frac{\phi_i \phi_j}{1 - \theta_i \theta_j}} \quad (3.18)$$

Process: Integrative

This process is defined as Equation 3.19. An integrative process is unstable ($z = 1$). Consequently, the mean value will be undefined and the theoretical autocorrelation, 1. In practice, it decays very slowly [22].

$$y_t = e_t + y_{t-1} = \frac{1}{1 - z^{-1}} e_t \quad (3.19)$$

Process: ARMA

The autoregressive, moving average process, **ARMA**(p,q), is defined by Equation 3.20. This process is causal⁴ if its **AR** component denominated by A -polynomial has its roots inside the unit circle. It will be called invertible⁵ if its **MA** component, denoted by B -polynomial, has its roots inside the unit circle [22].

$$y_t = \frac{B(z^{-1})}{A(z^{-1})} e_t = \frac{1 + \beta^{-1}z^{-1} + \beta_2 z^{-2} + \dots + \beta_q z^{-q}}{1 + \alpha_1 z^{-1} + \alpha_2 z^{-2} + \dots + \alpha_p z^{-p}} e_t \quad (3.20)$$

Process: ARIMA

Similarly to the **ARMA** process, the autoregressive, integrating, moving average process called **ARIMA**(p,d,q) is defined by Equation 3.21 [22].

$$y_t = \frac{B(z^{-1})}{A(z^{-1})(1 - z^{-1})^d} e_t = \frac{1 + \beta^{-1}z^{-1} + \beta_2 z^{-2} + \dots + \beta_q z^{-q}}{(1 + \alpha_1 z^{-1} + \alpha_2 z^{-2} + \dots + \alpha_p z^{-p})(1 - z^{-1})^d} e_t \quad (3.21)$$

3.1.3 Modeling Time Series

There are two steps to modeling a time series [22]:

⁴If an only if the current value can be determined with the current and past values [22].

⁵If and only if the inverse process is also casual: If $y_t = L e_t$ is casual and $e_t = L^{-1} y_t$ is casual \rightarrow process invertible [22].

1. Determining the model orders: Determines what kind of model is to be adopted.
2. Determining the model parameters: Provides the values needed for the model.

Time series modeling's procedure is summarized by Shardt [22] as the next steps:

1. **Stationary Testing:** Analyze the data and its autocorrelation to figure if the data set is indeed stationary.
2. **Model Order Determination:** Analyze the autocorrelation and partial autocorrelation plots to determine the order.
3. **Model Parameter Estimation:** Use the selected model order and appropriate method to determine parameters.
4. **Model Validation:** Validate the model by examining the residuals.

3.1.4 System Identification Methods

The middle ground between **FPM** and system identification as black-box is called grey-box modeling where the equation is formed by **FPM** and it is complemented by the data. Both the deterministic and the stochastic components of the model should be taken into account as shown in Equation 3.22 where u_t represents the deterministic input to the model, which can be handled like a time series and e_t is the disturbance signal [22].

$$y_t = f(\vec{u}_t, \vec{\beta}_u) + g(e_t, \vec{\beta}_e) \quad (3.22)$$

The prediction error model is the most general of plant models, represented by Equation 3.23. However, some simplifications can be made as: Box-Jenkins model shown in Equation 3.24, autoregressive moving average exogenous model (**ARMAX**) shown in Equation 3.25, autoregressive exogenous model (**ARX**) shown in Equation 3.26 and the output-error model (**OE**) shown in Equation 3.26 [22], [27], [28].

$$y_t = \frac{B(z^{-1})}{F(z^{-1})} u_{t-k} + \frac{C(z^{-1})}{D(z^{-1})} e_t \quad (3.23)$$

$$A(z^{-1})y_t = B(z^{-1})u_{t-k} + C(z^{-1})e_t \quad (3.24)$$

$$A(z^{-1})y_t = B(z^{-1})u_{t-k} + e_t \quad (3.25)$$

$$y_t = \frac{B(z^{-1})}{F(z^{-1})}u_{t-k} + e_t \quad (3.26)$$

System Identification Framework

The framework for system identification described by Shardt [22] consists of three steps:

1. **Data Collection:** Data is collected and analyzed. It is assumed that an experiment has been designed to obtain the adequate data. Design of experiments can be seen in subsection 3.4.2.
2. **Model Creation and Validation:** Data is used to create the model and find the parameter estimates and the model will be validated as shown in subsection 3.4.4.
3. **Decision Making:** It should be decided if the found model is sufficient or if a more suitable model is required.

3.2 Approximation in Mathematical Model Building

Models for real process will invariably involve some level of approximation, as Albert Einstein stated in German

“Soweit die Mathematik exakt ist, beschreibt sie nicht die Wirklichkeit, und soweit sie die Wirklichkeit beschreibt, ist sie nicht exakt”

which means “When the mathematics is exact, it fails to describe reality; when the mathematics describes reality, it is not exact”. Therefore, it is desirable to include knowledge of the degree of approximation into the design procedure, the additive modeling error (**AME**) and the multiplicative modeling error (**MME**) [11], [20], [29].

If the true plant is described by Equation 3.27 and its nominal model described by Equation 3.28, the **AME** will be defined by Equation 3.29 and the **MME** will be described by Equation 3.30 [11], [30].

$$y = g(u) \quad (3.27)$$

$$y_o = g_o(u) \quad (3.28)$$

$$y = y_o + g_\varepsilon(u) \quad (3.29)$$

$$y = g_o(u + g_{Delta}(u)) \quad (3.30)$$

3.3 Mathematical Model Types

In Table 3.1 in 38, a comprehensive list of mathematical model types, inspired on information from [6] is shown.

3.4 Model Considerations

3.4.1 Regression

Regression is the statistical process of estimating the relationship between a set of data and unknown parameter values by minimizing some criteria. Regression can be divided into linear regressions and nonlinear regression using either ordinary least-squares or weighted least-squares analysis [22].

A generalized representation of the regression problem is shown by Equation 3.31 where y is the output or dependent variable, g is the complete model, \vec{x} is an $l \times 1$ vector that contains the regressor or independent variables, $\vec{\beta}$ is an $n \times 1$ vector that contains the

Deterministic	Stochastic
Model works with an exact relationship between measurable and derived variables.	Model works with uncertainty. Contains quantities using stochastic variables.
Dynamic	Static
The variables change without direct outside influence. Values depend on earlier signals	Variables change with time. There is a direct link between the variables.
Continuous Time	Discrete Time
Describes relationships between time continuous signals. Often described by Differential Equations.	Describes relationships between values of signals at sampling instants. Often described by Difference Equations.
Lumped	Distributed
Events are described by a finite number of changing variables. Often described by ODE .	Events in the system are dispersed over the space variables. Often described by PDE .
Change Oriented	Discrete Event Driven
Described by continuous change. Correspond to the Newtonian paradigm in the model world.	Change takes place in terms of discrete events.

Table 3.1: Types of Mathematical Models [6]

parameters which are the model constants and ε is the error. To simplify calculation, the model g is divided into its deterministic component ($f(\vec{\beta}_x, \vec{x})$) known as the regression model and its stochastic component known ($k(\vec{\beta}_\varepsilon, \varepsilon)$) known as the error model [22].

$$y = g(\vec{\beta}, \vec{x}, \varepsilon) \quad (3.31)$$

There are two ways of including these components to the complete model:

1. Additive Approach
2. Multiplicative Approach

3.4.2 Design of Experiments

The objective is to design experiments so that the maximum information can be extracted and used in regression analysis. Various designs of the regression matrix \mathcal{A} will be developed. In general, the objective is to determine whether $\mathcal{A}^T \mathcal{A}$ is invertible and well conditioned [22].

3.4.3 Outlier Detection

Outliers are points that seem off and can be caused by different reasons, from data entry error to randomness in the system. Determining if a point is an outlier is subjective; however, there are some common rules [22].

1. Visual Test: Visual inspection to determine which values are far from the bulk of the data.
2. 3σ Edit Rule: Data points with Z -score as Equation 3.32.

$$Z_i = \frac{x_i - \mu}{\sigma} > 3 \quad (3.32)$$

3. Hampel Identifier: Points outside the band $x_{median} \pm 3\sigma_{mad}$ where σ_{mad} is defined by Equation 3.33.

$$\sigma_{mad} = 1.4826 \text{median}(|x_i - x_{median}|) \quad (3.33)$$

3.4.4 Model Validation

The difficulty in designing models lies in making them good and reliable. It is needed to have confidence in the result and predictions of the model for it to be useful. This confidence can be achieved by validating or verifying the model. In principle, model validation is done by comparing the model's behavior with the system's and evaluating the difference. All models have a domain of validity which corresponds to the accuracy demands and all models have a limited domain of validity and it is counterproductive to use a model outside its area of validity. It is important to remember that the model will

not be a perfect representation of reality nor should reality be forced to fit the model [6].

Three different components are considered when validating the model: testing the residuals, testing the model's adequacy and taking corrective action [22].

3.5 Framework for Physical Modeling

According to Ljung [6], there are three distinctive phases in order to find a mathematical model:

1. Problem is structured: The objective is to divide the system into subsystems in order to determine cause-effect relationships, the important variables and signals of interest to be considered outputs, and how they interact. The level of complexity and the degree of approximation is defined in this phase. The result is a diagram.
2. Equations are formulated: By examining the subsystems (blocks of phase 1) the relationships between variables and constants are formed by using physical and chemical equations. Some approximations or idealizations are made in order to avoid over-complicating the model.
3. Model is formed: Organization of equations and relationships found in phase 2. Simulations can be made in this phase.

It should be noted that the models, being simplifications of the real process, can be more simplified when the exact relationship between variables is unknown or if it has too many variables that it becomes unpractical to be useful. The simplification can be done in all the phases as described above [6].

4 Mathematical Model of Laboratory-Scale Distillation Column

4.1 Laboratory-Scale Distillation Column

In this section, the distillation column will be presented.

The distillation column to be modeled is part of the distillation plant located in the laboratory room Z1006 of the Zuse building, in the Institute of Automation and Systems Engineering of the Technical University of Ilmenau.

This plant, mainly used for training and research, separates ethanol from a mixture of ethanol and water in ten stages, in Figure 4.1 is a picture of the column and all its components.

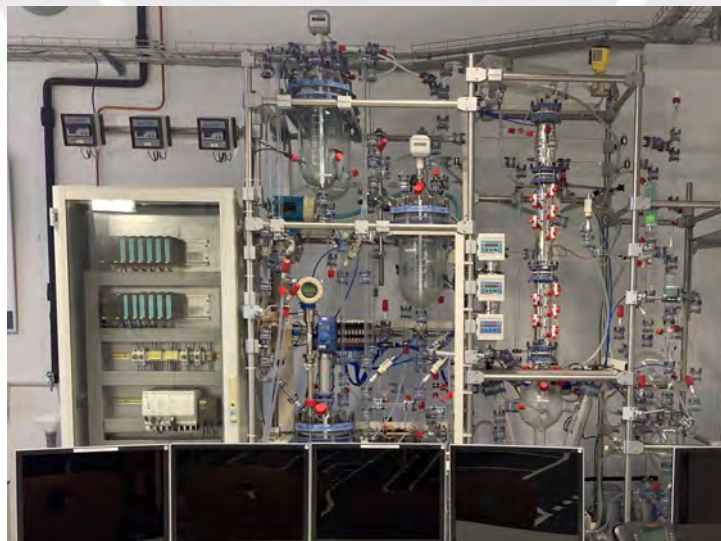


Figure 4.1: Picture of Ethanol-Water Distillation Plant

For the purpose of this thesis, the plant will be separated in three parts, as shown in Figure 4.2. The parts are: the mixing section (left side of the figure, inside the blue rectangle), the column (middle of the figure, in red) and receiver (right side of the figure, in green).

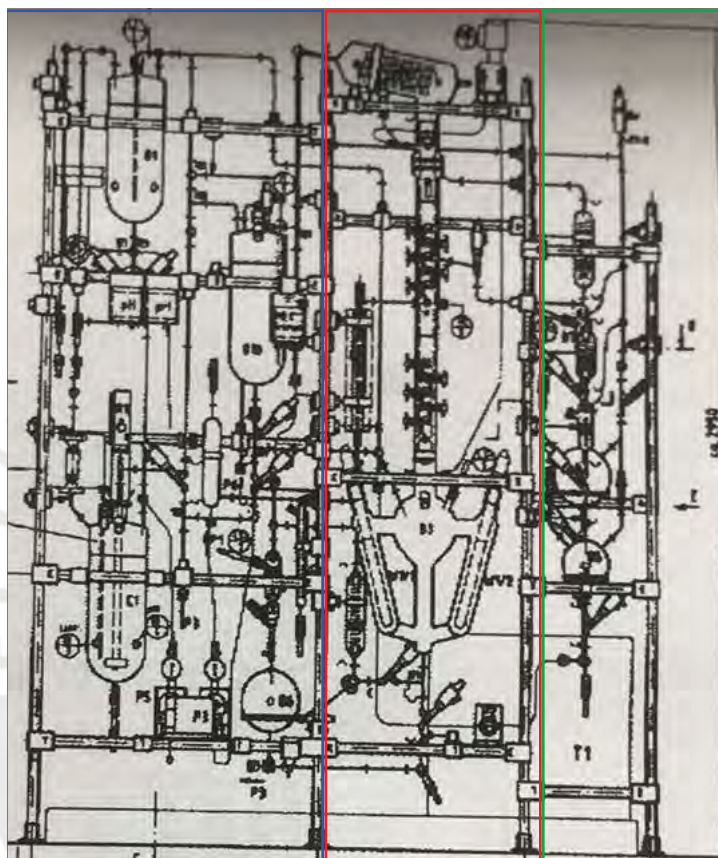


Figure 4.2: Diagram of Ethanol-Water Distillation Plant

The mixing section of the distillation plant consists of four see through tanks: B1 contains ethanol with unknown purity, B2 contains water with unknown purity, C1 is the mixing tank which contains the agitator and B10 contains the ethanol-water mixture that will be fed into the column.

The column part of the distillation plant contains the reboiler B3, condenser W2 and the bubble cap column, with its ten stages, *per se*.

The mixing section and the column can be seen in better detail in Figure 4.3.

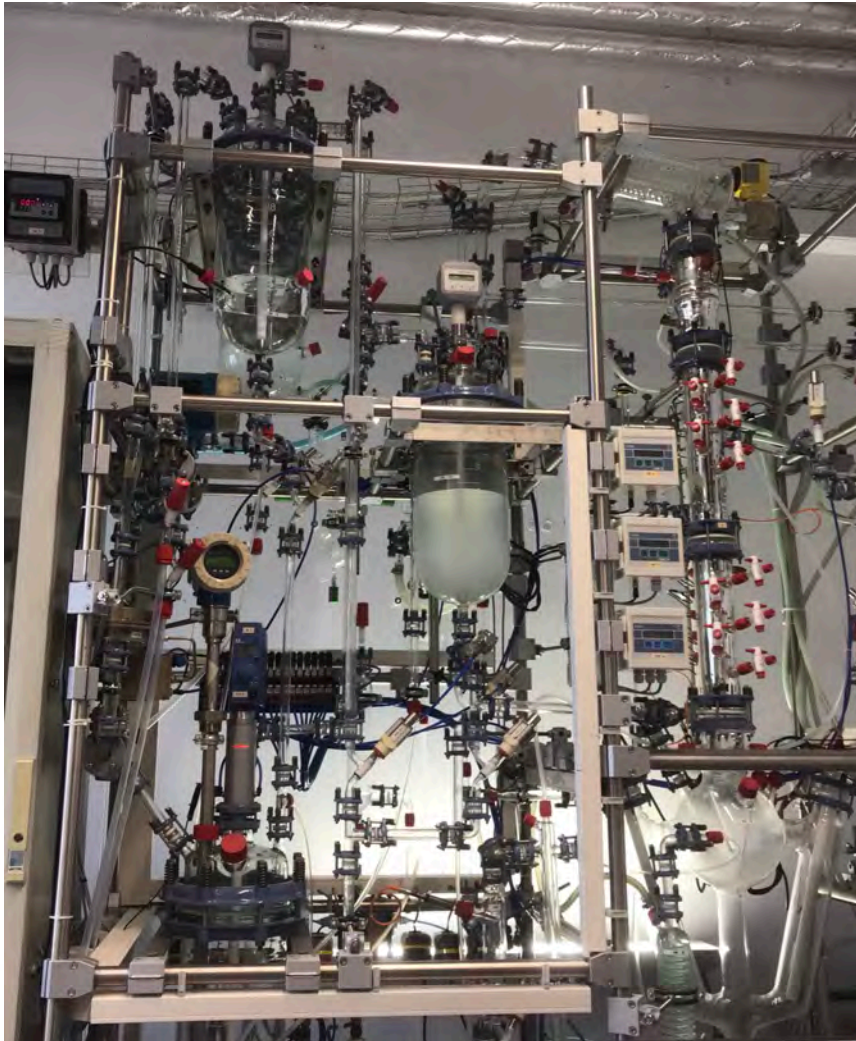


Figure 4.3: Mixing Section and Column of Ethanol-Water Distillation Plant

The receiver part has several receivers which serve to store the bottom product, the intermediate product and the distillate. The liquid from these receivers can be sent back to the column, either pumped into the bottom of the column or into the reboiler. The distillate can be withdrawn with some manual valves or returned to the column as reflux.

This plant has a controlled variable ΔP (differential pressure) and a manipulate variable T (temperature). The manipulated variable is affected by a switch off, switch on controller of two heating rods in the reboiler. The reference variable is the set differential pressure, which will in turn affect on the concentration of the distillate. In order to calculate the differential pressure, determined by *VEGADIF 34* [31], differential pressure

transmitter, the vapor pressure is measured both at the top of the column and in the reboiler and sent to the controller as a 4...20 mA signal.

The control system is implemented with the software *Freelance2000* from ABB [32]. In Figure 4.4 we can observe the entire Piping and Instrumentation Diagram (P&ID) of the distillation plant.

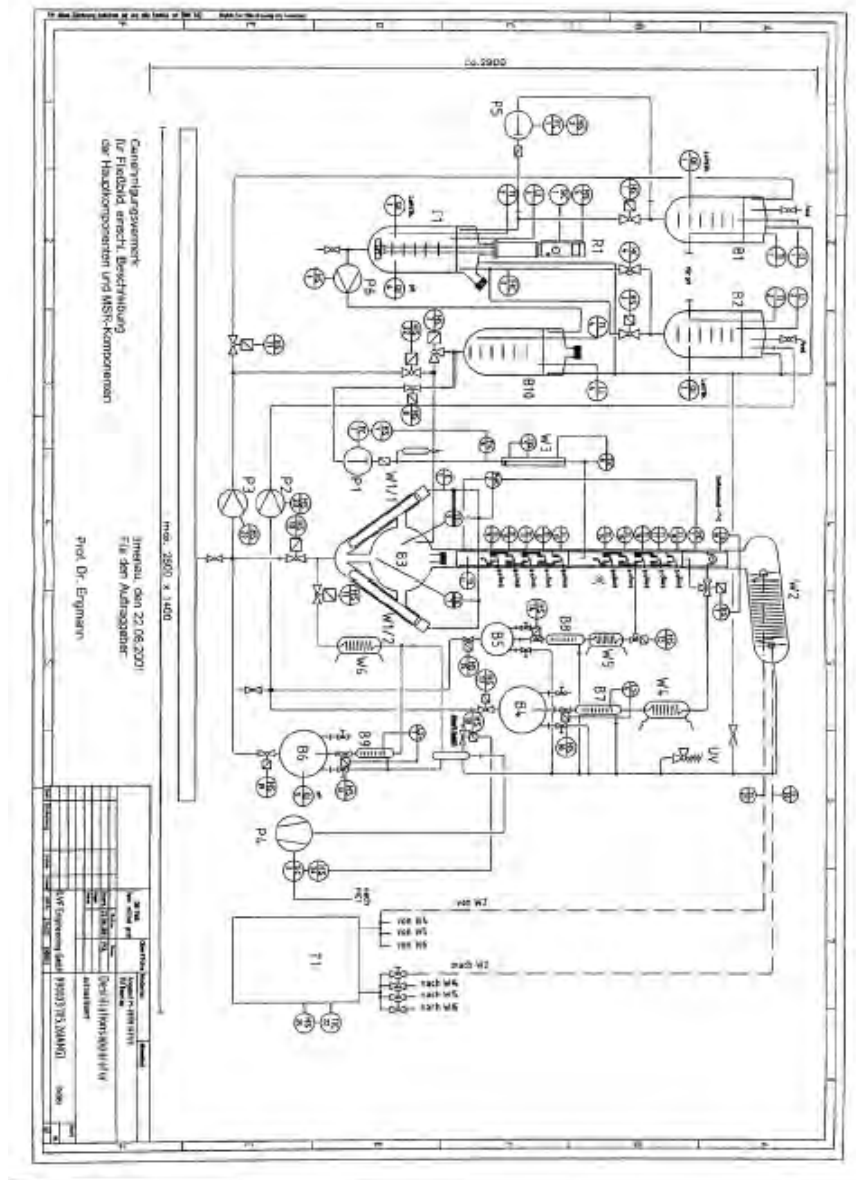


Figure 4.4: P&ID of Ethanol-Water Distillation Plant

4.1.1 Laboratory-Scale Distillation Column Process Control System

The Freelance2000 is a control system that is divided into control and process levels. The functions of the control level are operation and monitoring, archiving and logging, trend display and alarming. The functions of the process level are regulation, control and monitoring [32].

The control level consists of a control station (as an HMI¹/SCADA²) and an engineering station, both stations on separated computers. The engineering station, Freelance Engineering 2019, is used for configuring and commissioning the system.

The distributed control system consists of both computers, connected to the field controller via Ethernet, the field controller is, connected to the process decentralized peripherals via Profibus as shown in the Figure 4.5.

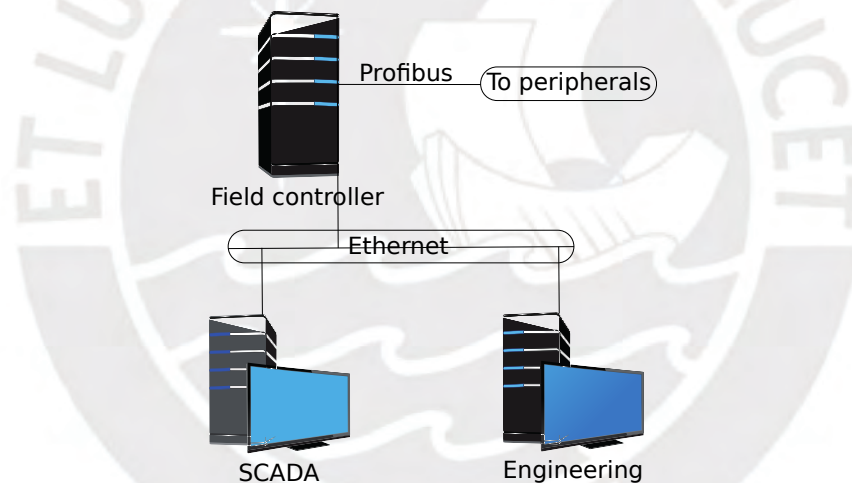


Figure 4.5: Hardware structure of the Process Control System

The HMI/SCADA is implemented in DigiVis500 [33], which allows the user to observe, operate and control the distillation plant. In Figure 4.6 is shown a graphic image of the distillation plant without showing the column.

¹Human Machine Interface

²Supervisory Control And Data Acquisition.

4.2. Laboratory-Scale Distillation Column Structure

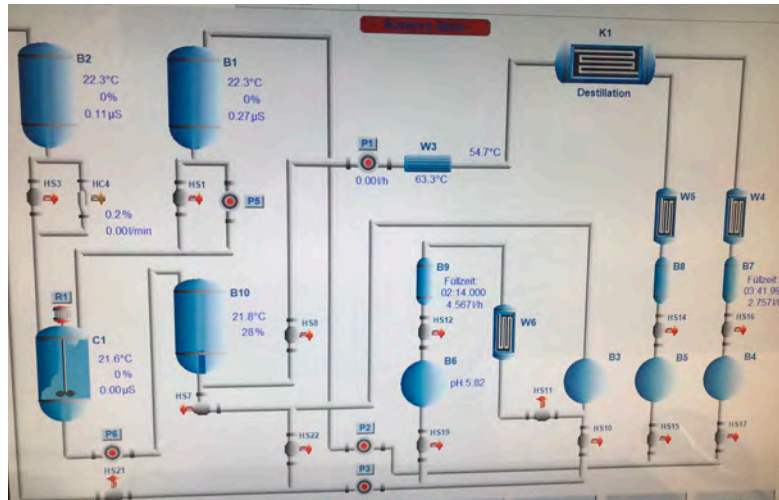


Figure 4.6: DigiVis - Distillation Plant without Column

In Figure 4.7 is shown the column and the continuously updated values of the variables read by the nearby temperature sensors.

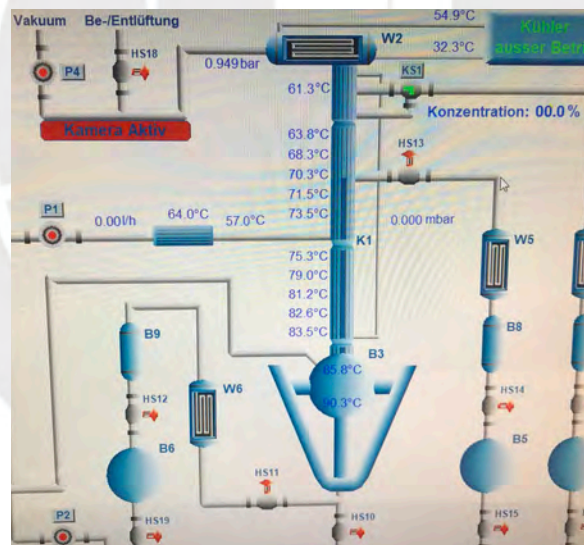


Figure 4.7: DigiVis - Distillation Plant with Column

4.2 Laboratory-Scale Distillation Column Structure

The focus of this thesis is the modeling of the distillation column *per se*. Figure 4.8 shows the condenser W2 (in blue), the column itself (in orange), the feed point F (in

purple) and the reboiler B3 (in green).

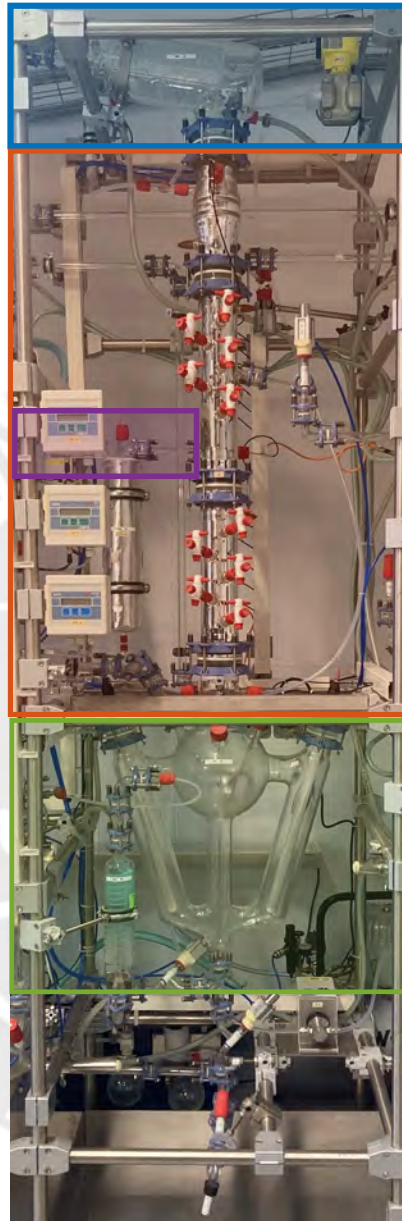


Figure 4.8: Column Structure

In order to follow the framework from section 3.5, the system is divided into subsystems. The subsystems are described in the following subsections.

4.2.1 Variables

The variables needed for the model can be divided into:

1. Inputs: External variables that can be manipulated, in this case:
 - a) R Reflux ratio;
 - b) Q_D Heat in the condenser;
 - c) Q_B Heat in the reboiler.
2. Disturbances: Other external inputs that can not be manipulated, in this case:
 - a) Contamination in the column;
 - b) Quantity of the feed;
 - c) Temperature of the feed;
3. Controlled Variables: Outputs of the system, in this case:
 - a) D Molar Flow rate of Distillate [mol/ min];
 - b) B Molar Flow rate of Bottom [mol/ min].
4. Process Variables: Those that are needed to describe the system but that are not inputs nor outputs, in this case:
 - a) M_B and M_D Holdup in reboiler and holdup in condenser;
 - b) L Molar Flow rate of Liquid [mol/ min];
 - c) V Molar Flow rate of Vapor [mol/ min];
 - d) F Molar Flow rate of Feed [mol/ min];
 - e) z Composition of the feed;
 - f) x_N Liquid concentration of the N stage [mol/mol];
 - g) y_N Vapor concentration of the N stage [mol/mol];
 - h) N Tray number.

4.2.2 Condenser

The total condenser is a heat exchanger which receives vapor from the column V , cools it with energy Q_C and then the cooled product is divided into reflux back to the column L and distillate D with a reflux ratio of R as shown in the Figure 4.9.

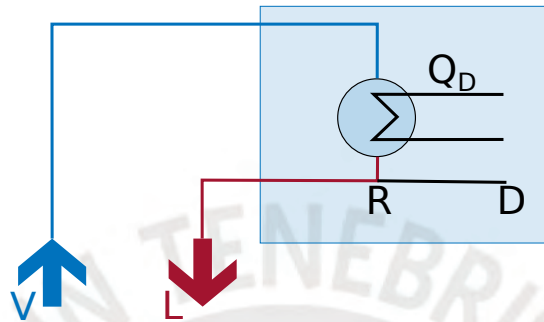


Figure 4.9: Diagram of the Condenser

A picture of the condenser is shown in Figure 4.10.



Figure 4.10: Picture of the Condenser

4.2.3 Column and Feedpoint

The column itself has ten stages. In Figure 4.11a it is shown a diagram of the column and in Figure 4.11b is a detailed diagram of an individual stage j .

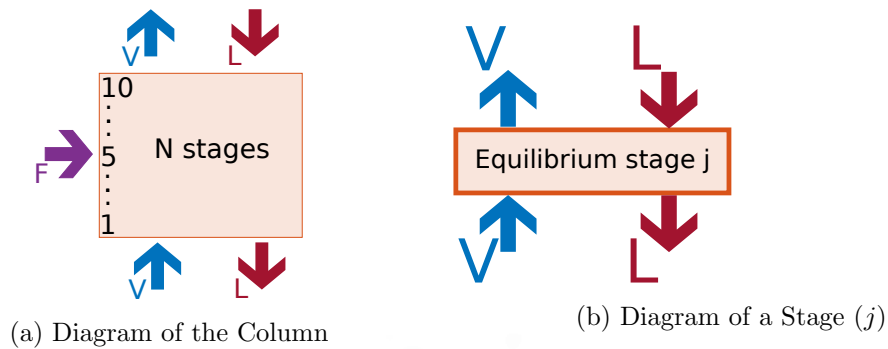


Figure 4.11: (a) Diagram of the Column (b) Diagram of a Stage (j)

The feed point F is located in the middle of the column (5th stage) and shown in Figure 4.12.

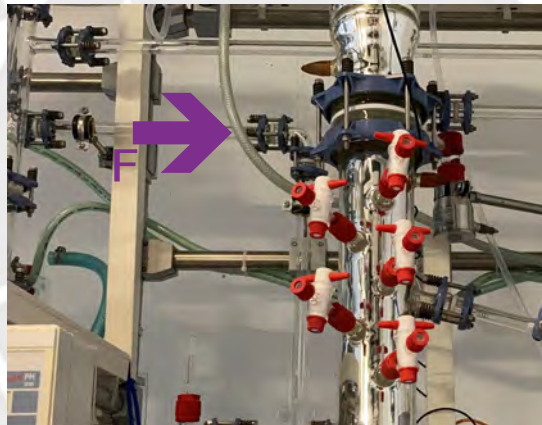


Figure 4.12: Picture of the Feed Point

4.2.4 Reboiler

The reboiler is also a heat exchanger which receives liquid from the column L , heats it with energy Q_B and then the heated product is divided into V that goes back to the column and B , the bottoms product as shown in Figure 4.13.

The reboiler is heated by two rods, as seen in Figure 4.14 with 1.5 [kW] each rod.

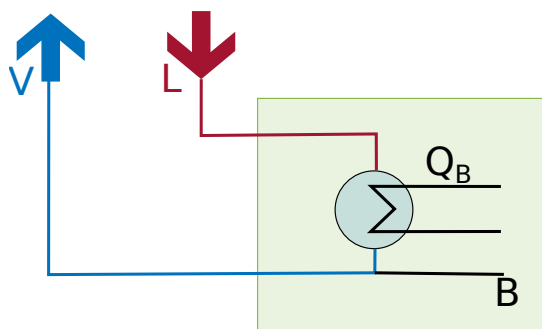


Figure 4.13: Diagram of the Reboiler



Figure 4.14: Picture of the Reboiler

4.3 Laboratory-Scale Distillation Column Assumptions

The assumptions from Section 2.10 are taken into account and the total list of assumptions made are:

1. Constant molar overflow (heat losses from the column and from mixing are insignificant, the molar latent heat of vaporization of the two components is similar, and the boiling point of the liquid does not change significantly across the column);
2. For every liquid mole vaporized, a mole of vapor is condensed;
3. Each stage is in phase equilibrium and perfectly mixed³;
4. There are no chemical reactions happening in a stage;

³The liquid composition is homogeneous.

5. Liquid droplets in vapor and vapor bubbles in liquid are negligible;
6. There are no starting or shutting down process;
7. There is no switching between different stationary operating points.

4.4 Laboratory-Scale Distillation Column Equations

4.4.1 Condenser

The vapor coming from the column is completely condensed with heat Q_D . The distillate coming from the condenser is collected in different receivers.

Material Balance:

$$\frac{dM_D}{dt} = V_{10} - R - D \quad (4.1)$$

Since it is totally condensed, V_{10} is considered equal to 0.

Component Material Balance:

$$\frac{d(M_D x_D)}{dt} = V_{10} y_{10} - (R + D) x_D \quad (4.2)$$

Rewriting the equation 4.2:

$$\frac{d(x_D)}{dt} = \frac{V_{10} y_{10} - (R + D) x_D}{M_D} \quad (4.3)$$

We also have the equities:

$$L_{10} = (1 - R) V_{10} \quad (4.4)$$

$$D = V_{10} - L_{10} \quad (4.5)$$

Equation 4.4 and Equation 4.5 give way to Equation 4.6:

$$D = R V_{10} \quad (4.6)$$

Replacing Equation 2.55 from section 2.11 and Equation 4.6 in Equation 4.3, the condenser dynamics are represented by nonlinear Equation 4.7:

$$\frac{d(x_D)}{dt} = \frac{V_{10}}{M_D} \left(\frac{\alpha_{10} x_{10}}{1 - (\alpha_{10} - 1) x_{10}} \right) - \frac{L_{10} x_D}{M_D} - \frac{R V_{10} x_D}{M_D} \quad (4.7)$$

Mole Fraction Summations:

$$\sum_{i=1}^2 x_{i,10} = 1 \quad (4.8)$$

$$\sum_{i=1}^2 y_{i,10} = 1 \quad (4.9)$$

Energy Balance:

$$\frac{d(M_D H_D)}{dt} = V_{10} H_{10}^V - (R + D) H_D^L + Q_D \quad (4.10)$$

4.4.2 Column and Feed Point

Top tray material balance:

$$\frac{dM_9}{dt} = R - L_9 \quad (4.11)$$

Top tray component material balance:

$$\frac{d(M_9 x_9)}{dt} = R x_D - L_9 x_9 + V_9 y_9 - V_{10} y_{10} \quad (4.12)$$

Rewriting Equation 4.12:

$$\frac{d(x_9)}{dt} = \frac{R x_D - L_9 x_9 + V_9 y_9 - V_{10} y_{10}}{M_9} \quad (4.13)$$

Replacing Equation 2.55 in Equation 4.13, the top tray dynamics are represented by nonlinear Equation 4.14:

$$\frac{d(x_9)}{dt} = \frac{R x_D}{M_9} - \frac{L_9 x_9}{M_9} + \frac{V_9}{M_9} \left(\frac{\alpha_9 x_9}{1 - (\alpha_9 - 1) x_9} \right) - \frac{V_{10}}{M_9} \left(\frac{\alpha_{10} x_{10}}{1 - (\alpha_{10} - 1) x_{10}} \right) \quad (4.14)$$

Material balance for the next tray:

$$\frac{dM_8}{dt} = L_9 - L_8 \quad (4.15)$$

Component material balance for the next tray:

$$\frac{d(M_8 x_8)}{dt} = L_9 x_9 - L_8 x_8 + V_8 y_8 - V_9 y_9 \quad (4.16)$$

Therefore, the material balance and the component material balance for each stage j , where $j = \{j \in \mathbb{N}; 1 < j < 10\}$, can be written as Equations 4.17 and 4.18:

Material Balance:

$$\frac{dM_j}{dt} = L_{j+1} - L_j \quad (4.17)$$

Component Material Balance:

$$\frac{dM_j x_j}{dt} = L_{j+1} x_{j+1} - L_j x_j + V_j y_j - V_{j+1} y_{j+1} \quad (4.18)$$

Rewriting Equation 4.18:

$$\frac{dx_j}{dt} = \frac{L_{j+1} x_{j+1} - L_j x_j + V_j y_j - V_{j+1} y_{j+1}}{M_j} \quad (4.19)$$

Replacing Equation 2.55 in Equation 4.19, the tray dynamics are represented by nonlinear Equation 4.20:

$$\frac{dx_j}{dt} = \frac{L_{j+1} x_{j+1}}{M_j} - \frac{L_j x_j}{M_j} + \frac{V_j}{M_j} \left(\frac{\alpha_j x_j}{1 - (\alpha_j - 1) x_j} \right) - \frac{V_{j+1}}{M_j} \left(\frac{\alpha_{j+1} x_{j+1}}{1 - (\alpha_{j+1} - 1) x_{j+1}} \right) \quad (4.20)$$

For the feed tray material balance:

$$\frac{dM_5}{dt} = F + L_6 - L_5 \quad (4.21)$$

Feed tray component material balance:

$$\frac{d(M_5 x_5)}{dt} = L_6 x_6 - L_5 x_5 + V_5 y_5 - V_6 y_6 + Fz \quad (4.22)$$

The feed tray dynamics are represented by:

$$\frac{d(x_5)}{dt} = \frac{L_6 x_6}{M_5} - \frac{L_5 x_5}{M_5} + \frac{V_5}{M_5} \left(\frac{\alpha_5 x_5}{1 - (\alpha_5 - 1) x_5} \right) - \frac{V_6}{M_5} \left(\frac{\alpha_6 x_6}{1 - (\alpha_6 - 1) x_6} \right) + \frac{Fz}{M_5} \quad (4.23)$$

Energy Balance:

$$\frac{d(M_j H_j)}{dt} = L_{j+1} H_{j+1}^L - L_j H_j^L + V_j H_j^V - V_{j+1} H_{j+1}^V \quad (4.24)$$

Mole Fraction Summations:

$$\begin{aligned} \sum y_i &= 1 \\ \sum x_i &= 1 \end{aligned} \quad (4.25)$$

4.4.3 Reboiler

Material Balance:

$$\frac{dM_B}{dt} = L_1 - V_1 - B \quad (4.26)$$

Component Material Balance:

$$\frac{d(M_B x_B)}{dt} = L_1 x_1 - V_1 y_1 - B x_B \quad (4.27)$$

We also have the next equity:

$$L_1 = V_1 + B \quad (4.28)$$

Replacing L_1 from Equation 4.28 in Equation 4.27:

$$\frac{d(x_B)}{dt} = \frac{V_1(x_1 - y_1)}{M_B} + \frac{B(x_1 - x_B)}{M_B} \quad (4.29)$$

Mole Fraction Summations:

$$\sum_{i=1}^2 x_{i,10} = 1 \quad (4.30)$$

$$\sum_{i=1}^2 y_{i,10} = 1 \quad (4.31)$$

Energy Balance:

$$\frac{d(M_B H_B)}{dt} = L_1 H_1^L + Q_B - V_1 H_1^V - B H_B^L \quad (4.32)$$

For the Heat Exchanger:

$$Q_B = V (H_{ethanol}^{vap} x_1 + H_{water}^{vap} (1 - x_1)) \quad (4.33)$$

where Q_B is the heat power [W], $H_{ethanol}^{vap}$ is the ethanol vaporization energy and H_{water}^{vap} is the water vaporization energy.

Replacing V from Equation 4.33 in Equation 4.29, the dynamics of the reboiler are described in Equation 4.34:

$$\frac{d(x_B)}{dt} = \left[\frac{Q_B}{(H_{ethanol}^{vap} x_1 + H_{water}^{vap} (1 - x_1))} \left(\frac{x_1}{M_B} \right) \left(\frac{1 - \alpha_1}{1 - (\alpha_1 - 1)x_1} \right) \right] + \frac{B(x_1 - x_B)}{M_B} \quad (4.34)$$

4.5 Laboratory-Scale Distillation Column Model

The complete diagram of the distillation column is shown in Fig. 4.15.

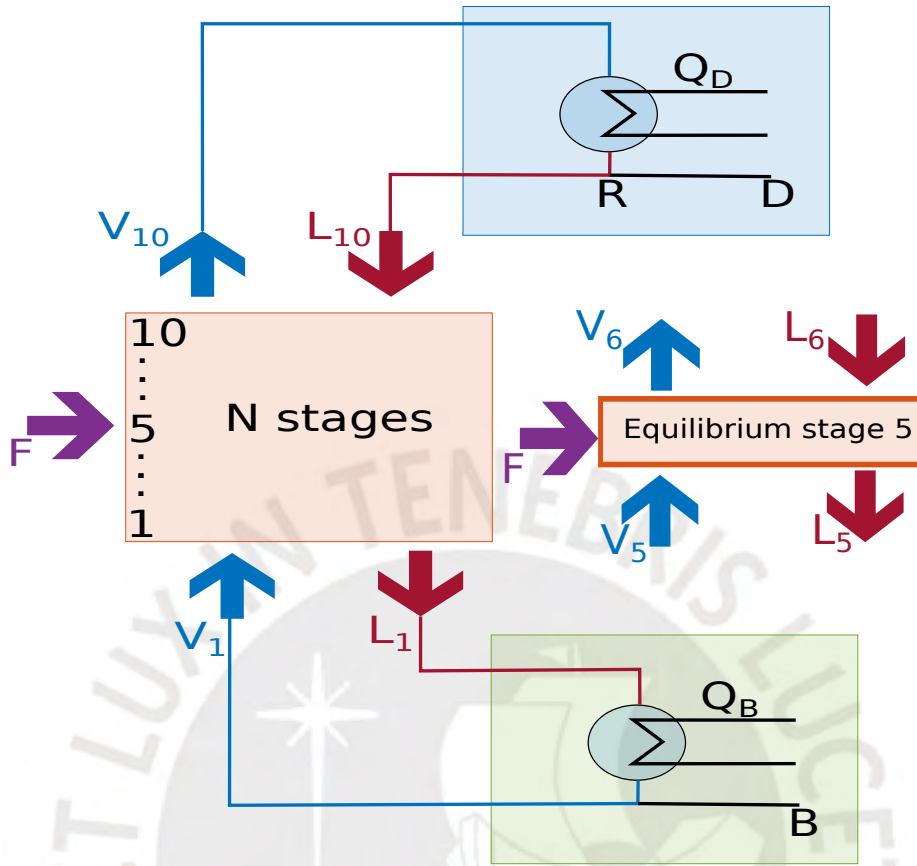


Figure 4.15: Complete diagram of the column

In order to link these equations with pressure (P) and temperature (T), it is important to remember that the phases are in chemical equilibrium, which means they hold the same temperature and pressure, this can also be described by the equality of fugacities as seen in Equation 4.35.

$$f_i^L = f_i^V, \quad (4.35)$$

where f_i^L is the fugacity of the component i in liquid phase and f_i^V in vapor phase. Based on the phase equilibrium equation (Equation 4.40) and the fugacity equation (Equation 2.36), the phase equilibrium ratio K_i can be written as:

$$K_i = \frac{\gamma_i \phi_i^{sat} P_i^{sat}}{\hat{\phi}_i^V} \exp \left(\int_{P_i^{sat}}^P \frac{V_i^L}{RT} dP \right), \quad (4.36)$$

where $\hat{\phi}_i^V$ is the fugacity of the component i in vapor phase, ϕ_i^{sat} is the fugacity coefficient of the component i in saturation state, P^{sat} is the saturated vapor pressure, V_i^L is the volume of the component i in liquid phase and the other variables are as previously defined.

The fugacity coefficient is calculated using an equation of state, and the activity coefficient is calculated using the Gibbs free energy.

4.6 Laboratory-Scale Distillation Column Model Simplification

The complete MESH equations for the column are as follows:

Total mass balance: Found by adding up all the material balances

$$F = D + B \quad (4.37)$$

Total energy balance: Calculated analogously to the total mass balance

$$FH^F + Q_B + Q_D = (BH_B^L + DH_D^L) \quad (4.38)$$

Mole Fraction Summations:

$$\begin{aligned} \sum_{j=1}^n y_j &= 1 \\ \sum_{j=1}^n x_j &= 1 \end{aligned} \quad (4.39)$$

Phase equilibrium Equation:

$$y_j - K_j x_j = 0, \quad (4.40)$$

where K is the phase equilibrium ratio.

System Dynamics:

$$\begin{aligned} \dot{x}_D &= \frac{V_{10}}{M_D} \left(\frac{\alpha_{10} x_{10}}{1 - (\alpha_{10} - 1)x_{10}} \right) - \frac{L_{10} x_D}{M_D} - \frac{RV_{10} x_D}{M_D} \\ \dot{x}_9 &= \frac{Rx_D}{M_9} - \frac{L_9 x_9}{M_9} + \frac{V_9}{M_9} \left(\frac{\alpha_9 x_9}{1 - (\alpha_9 - 1)x_9} \right) - \frac{V_{10}}{M_9} \left(\frac{\alpha_{10} x_{10}}{1 - (\alpha_{10} - 1)x_{10}} \right) \end{aligned}$$

The differential variables \dot{x}_8 , \dot{x}_7 , \dot{x}_6 follow the shape of Equation 4.41

$$\begin{aligned}\dot{x}_j &= \frac{L_{j+1}x_{j+1}}{M_j} - \frac{L_jx_j}{M_j} + \frac{V_j}{M_j} \left(\frac{\alpha_jx_j}{1 - (\alpha_j - 1)x_j} \right) - \frac{V_{j+1}}{M_j} \left(\frac{\alpha_{j+1}x_{j+1}}{1 - (\alpha_{j+1} - 1)x_{j+1}} \right) \quad (4.41) \\ \dot{x}_5 &= \frac{L_6x_6}{M_5} - \frac{L_5x_5}{M_5} + \frac{V_5}{M_5} \left(\frac{\alpha_5x_5}{1 - (\alpha_5 - 1)x_5} \right) - \frac{V_6}{M_5} \left(\frac{\alpha_6x_6}{1 - (\alpha_6 - 1)x_6} \right) + \frac{Fz}{M_5}\end{aligned}$$

The differential variables \dot{x}_4 , \dot{x}_5 , \dot{x}_2 and \dot{x}_1 also follow the shape of Equation 4.41.

$$\dot{x}_B = \left[\frac{Q_B}{(H_{ethanol}^{vap}x_1 + H_{water}^{vap}(1 - x_1))} \left(\frac{x_1}{M_B} \right) \left(\frac{1 - \alpha_1}{1 - (\alpha_1 - 1)x_1} \right) \right] + \frac{B(x_1 - x_B)}{M_B}$$



5 Simulation of the Laboratory-Scale Distillation Column

Simulating the system will mainly help to have a better understanding of it and predict its behavior when there's a change in the inputs. And also to know how is it affected by the external influences of the stochastic variables on the feed stream.

5.1 Variables

Input Variables:

- Q_D Condenser heat
- Q_B Reboiler heat
- R Reflux ratio

Process Variables:

- M_D Holdup in the condenser
- M_B Holdup in the reboiler
- x_B Bottoms desired composition (> 0.05)
- x_D Distillate desired composition (< 0.95)
- $[F, z, qF]$ Feed molecular flow, feed composition and feed quality

Outputs of the system

- D Distillate flow
- B Bottoms flow

5.2 Assumptions for Simulation

Several runs of the simulation with different values were made in order to obtain the results later shown. Table 5.1 shows the ones that were assumed to run the future simulations.

Variable	Assumed Value
L along the column	2.65
V along the column	3.12
M_D	0.5
M_B	0.5
x_B	0.1
x_D	0.9
$[F, z, qF]$	$[1, 0.5, 1]$

Table 5.1: Assumed values of variables needed for simulation

5.3 Simulation Results

For the Simulink model, the function *model* is defined in Matlab with inputs of the heat, the desired concentrations of bottom product and distillate, and the assumed values for the feed. The outputs, as previously mentioned are D and B and are exported as variables to Matlab. In Figure 5.1 is shown the model used to achieve this.

The modeled temperatures along the distillation column can be seen in Figure 5.2. It can be seen that the stages tend to maintain its initial value (22.3°C) until the vapor rises enough and the temperature quickly reaches a higher temperature (higher than the ethanol boiling point but lower than the water boiling point). It can be seen that it takes approximately 50 seconds for the distillate to be available, the delays in the rising time were fixed to match the experimental values.

The model shown in Figure 5.3 was used to export the values of the vapor composition (y_B [mol/mol]) and the liquid composition (x_D [mol/mol]) to the workspace in Matlab using the function *modelFor_x_y*.

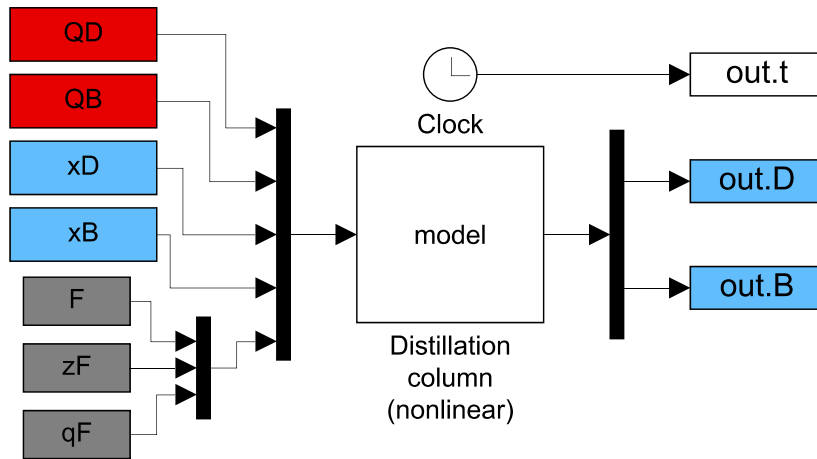


Figure 5.1: Simulink Model of the Distillation Column

The plate efficiency η determines the effectiveness of a separation stage and can only be determined by empirical methods, which makes it a stochastic variable which could be better determined by several experiments. This thesis considered η as 100%.

Figure 5.4 shows the mole fraction of ethanol in the liquid phase per stage according to the model, data which will later be compared with the McCabe-Thiele diagram in Section 6.1. It can be seen that for the first stage, it uses the composition of the bottom product x_B at 0.1[mol/mol].

Figure 5.5 shows the mole fraction of ethanol in the vapor phase per stage according to the model. This data will later be compared with the McCabe-Thiele diagram in Section 6.1. There is no fixed initial value for the vapor mole fraction since it will depend on the value of x_B and the **VLE** curve.

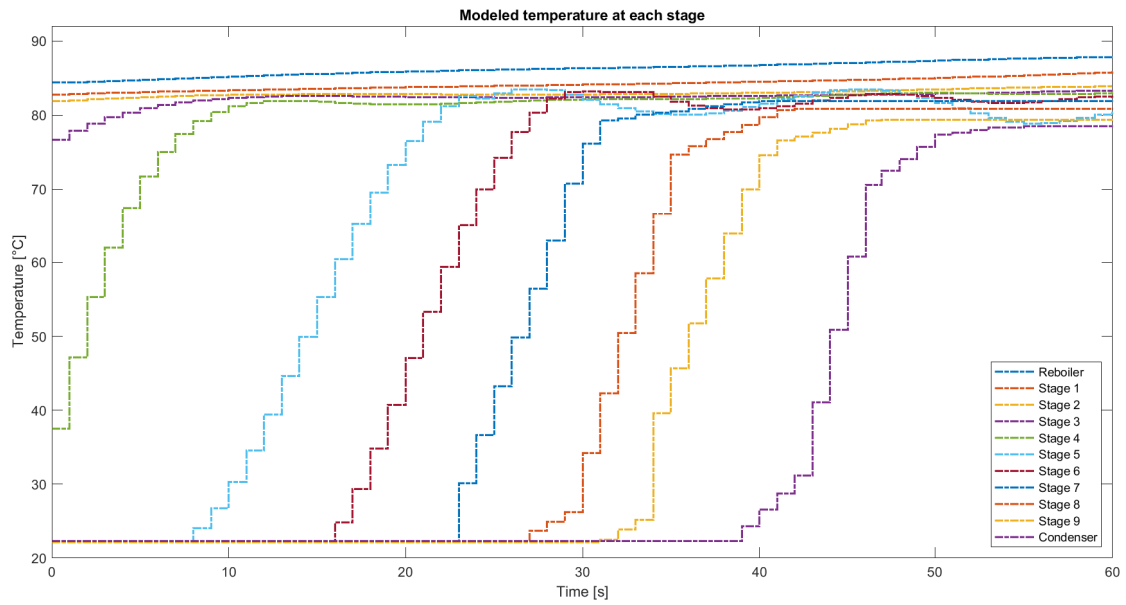


Figure 5.2: Modeled temperature at each stage

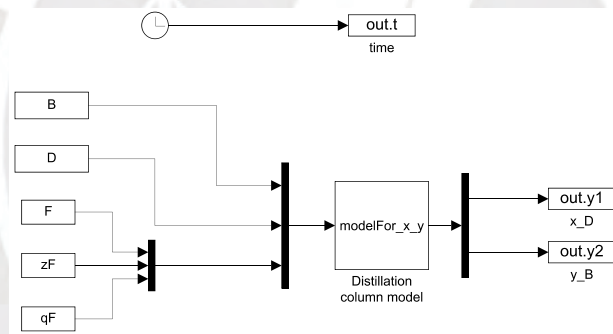


Figure 5.3: Simulink Model for x_D and y_B

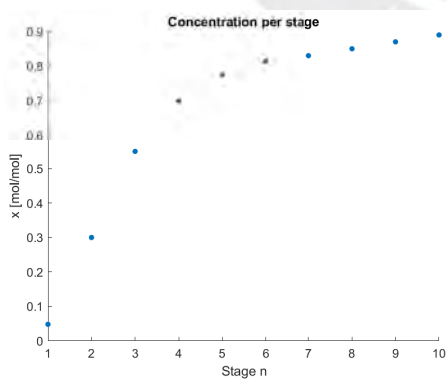


Figure 5.4: x per stage

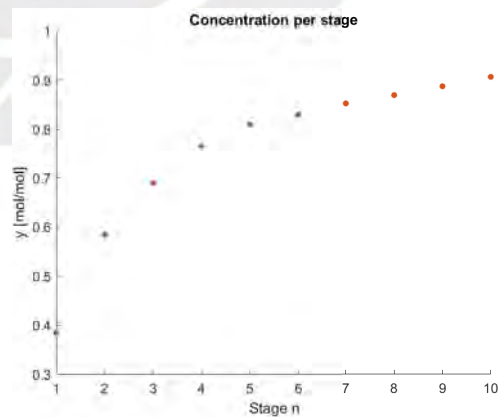


Figure 5.5: y per stage

6 Comparison of Distillation Column and Nominal Model

The suggested model will be compared with the results from using the McCabe-Thiele diagram and with the temperatures measured in the laboratory.

6.1 Comparison against the McCabe-Thiele method

In order to use the McCabe-Thiele diagram it is necessary to plot the vapor-liquid equilibrium (**VLE**) data. This data was obtained from [4].

Figure 6.1 shows the **VLE** for a mixture of ethanol and water at different pressures. It can be seen that the difference in pressure only affects the area with low concentrations of liquid ethanol (< 0.2 mol/mol).

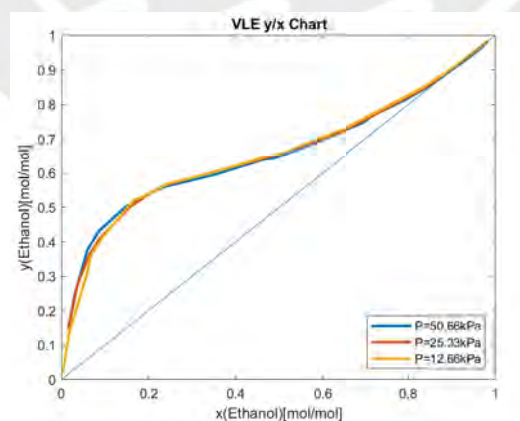


Figure 6.1: **VLE** of Ethanol and Water [4].

The **VLE** also give us information about the relative volatility of the components following the formula:

$$\alpha = \frac{y}{x} \left(\frac{1-x}{1-y} \right) \quad (6.1)$$

The corresponding α for each pressure was then plotted in Figure 6.2. It can be seen that, for the higher pressures (25.33 kPa and 50.66 kPa), the behavior of α is similar and follows the same decaying tendency, while for the lower pressure (12.66 kPa) it does not follow the same tendency.

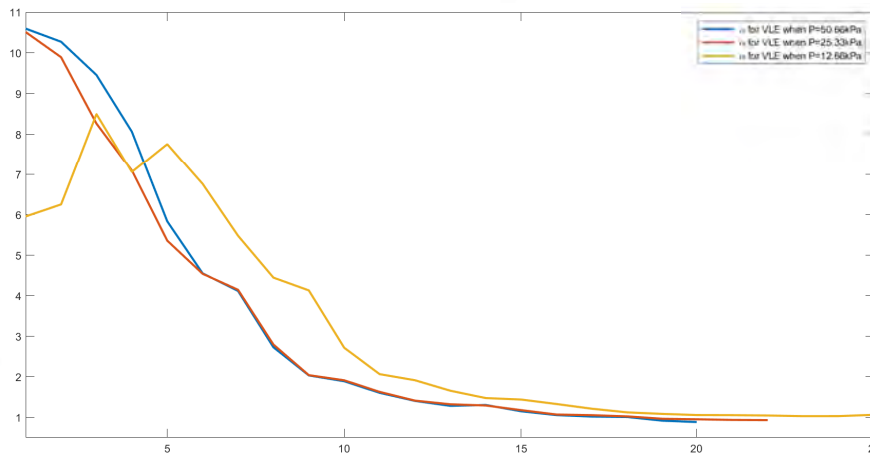


Figure 6.2: α value for different pressures

The temperature of the feed cannot be controlled. However, it can be measured and for this thesis it was considered to be around 60°C according to the McCabe-Thiele method, the minimum number of stages needed to achieve the separation of ethanol and water at this temperature and 50 kPa is 8 and the minimum reflux ratio is 2.12.

A program is developed in Matlab in order to plot the McCabe-Thiele diagram. Since the working pressure is set and the column has 10 trays, a reflux ratio of 10 was chosen. The list of values used to plot the diagram are shown in Table 6.1.

Variable	x_B	x_D	Reflux ratio	z	q_F
Value	0.1	0.9	10	0.5	1

Table 6.1: McCabe-Thiele Diagram Values

The McCabe-Thiele diagram plotted for the **VLE** of ethanol and water is shown in

Figure 6.3. It can be seen that for the input values the number of stages is, indeed, ten.

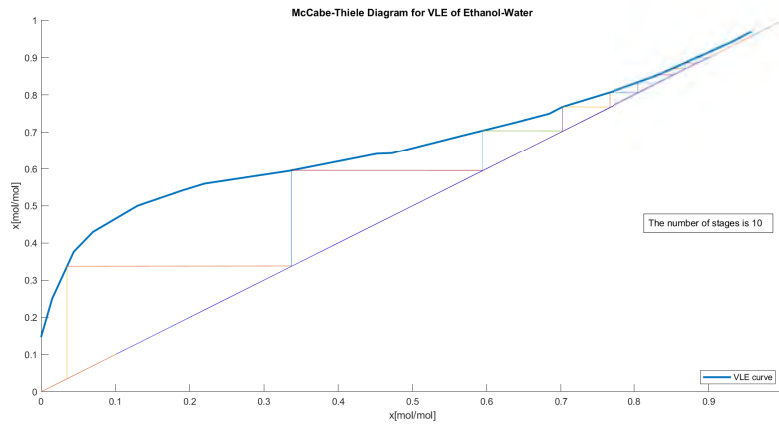


Figure 6.3: McCabe-Thiele Diagram for **VLE** of ethanol-water

The values of x_j and y_j for the more volatile component (ethanol) are taken from the McCabe-Thiele diagram, as shown in Figure 6.4.

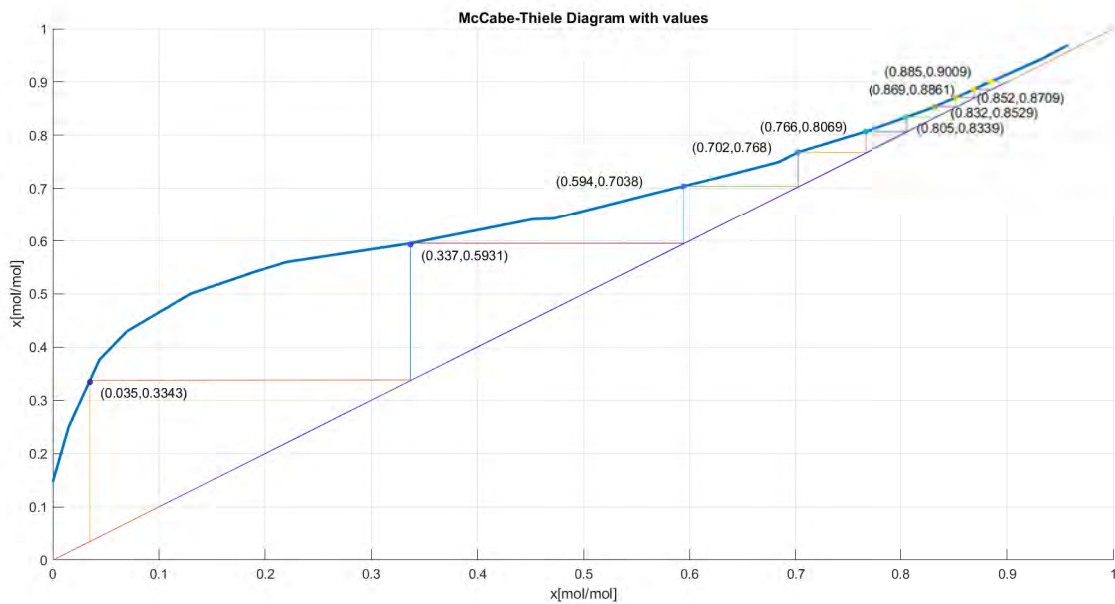


Figure 6.4: McCabe-Thiele Diagram with values for x_j and y_j

Figure 6.5 shows the comparison of the mole fraction of ethanol in the liquid phase (in Figure 5.4) from the model with the data from the McCabe-Thiele diagram. It is seen that, for the simulated parameters, the error between both mole fractions is considerably small. The mean of the error $\mu_{error} = 0.0052$. The maximum error for the mole fraction in the liquid phase is 0.044, which comparing to the value of stage 3, is an error of 7.4%. It is also noted that both initial concentrations $x_{1McT} = 0.035$ mol/mol and $x_{1Sim} = 0.048$ mol/mol are smaller than the required $x_B = 0.1$, the error is greater in the first stages since the concentration is mostly influenced by the assumptions of the feed concentration and initial conditions of the column. However, for the top of the column the final concentrations are $x_{10McT} = 0.885$ mol/mol and $x_{10Sim} = 0.890$ mol/mol the values are much closer to the required value of $x_D = 0.9$. Where n_{McT} is the subscript for the stage n in the McCabe-Thiele diagram and n_{Sim} for the simulation.

Analogously, Figure 6.6 shows the comparison of the mole fraction of ethanol in vapor phase (in Figure 5.5) from the model with the data from the McCabe-Thiele diagram. In this case the concentrations do not share a starting point which makes the error in the beginning of the column bigger (0.05), however still acceptable. It is also noted that both initial concentrations $y_{1McT} = 0.334$ mol/mol and $y_{1Sim} = 0.384$ mol/mol differ in 14% since there is no shared starting point. However this does not affect the overall simulation since for the top of the column the final concentrations are $y_{10McT} = 0.901$ mol/mol and $y_{10Sim} = 0.9060$ mol/mol the error here is 1% and the mean of the error along the column is $\mu_{error} = 0.0028$.

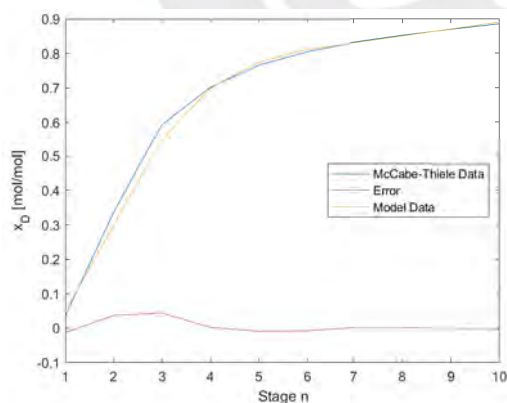


Figure 6.5: Comparison of x per stage between McCabe-Thiele Diagram and Suggested Model

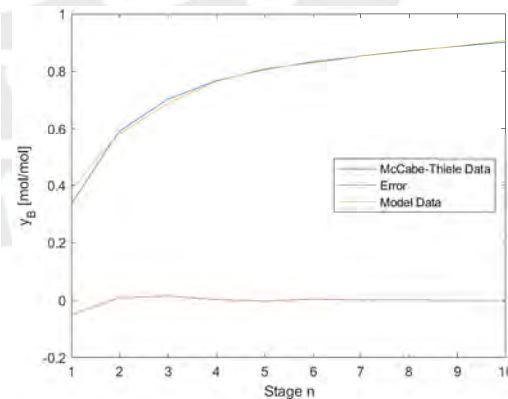


Figure 6.6: Comparison of y per stage between McCabe-Thiele Diagram and Suggested Model

6.1. Comparison against the McCabe-Thiele method

These values are then plotted against the **VLE** curve in two separated plots (for better visualization of the high mole fractions). Figure 6.7 shows the molar fractions corresponding to stages 1 to 4. Figure 6.8 shows the values corresponding to stages 5 to 10.

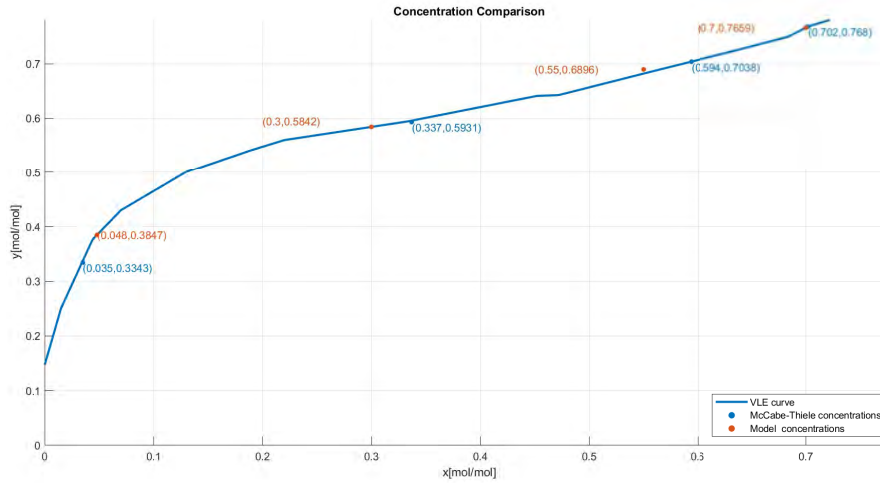


Figure 6.7: Concentration Comparison for Stages 1 to 4

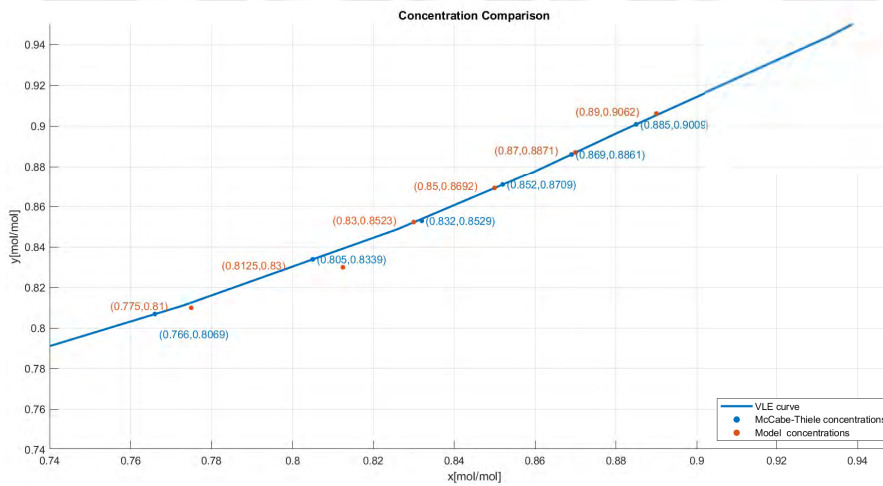


Figure 6.8: Concentration Comparison for Stages 5 to 10

As seen in the previous figures, the mole fractions from the model are close to the **VLE**

curve, with exceptions of stages 5 and 6 which were more influenced by the feed composition z .

6.2 Comparison against experimental temperatures

Data from the temperature from one run in the distillation plant was available and plotted in Figure 6.9.

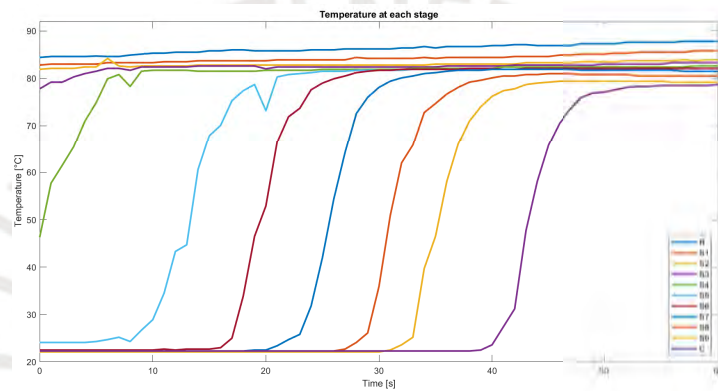


Figure 6.9: Temperature at each stage

Since the measured values of the temperature are not continuous but rather events in time which is why the data is plotted again with a zero-order hold in Figure 6.10.

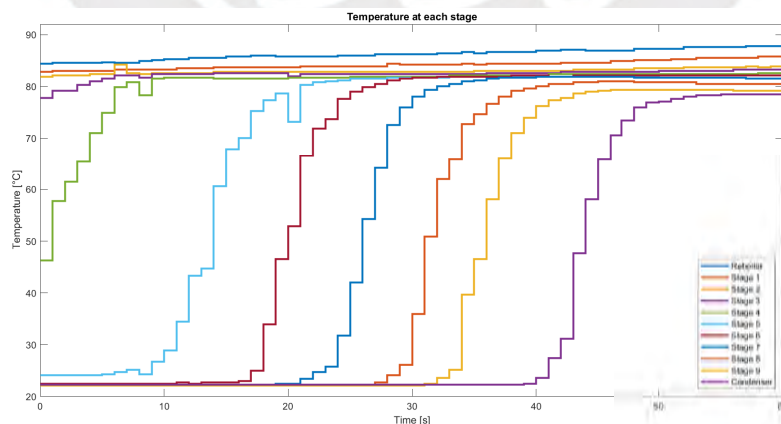


Figure 6.10: Temperature at each stage after zero-order hold

It can be seen that the temperatures at stage 4 (S_4) and stage 5 (S_5) are the ones that most differ from the expected value because stage 5 is directly in contact with the incoming feed temperature and being the incoming stream in the liquid phase, most of the feed will flow downward.

Figure 6.11 shows a comparison between the real data of the temperature (in blue) and the modeled data of the temperature (in orange) at stages 1 to 4. It can be noted that the proposed model for these stages, the ones closer to the reboiler and below the feed point, follows the tendency of the real data. In stage 2, there is a small peak around the 8 seconds which, for modeling purposes, was considered an outlier and ignored. It can be seen that for the bottom tray the final temperatures, $T_{f1Mod} = 85.6^\circ\text{C}$ and $T_{f1Exp} = 85.8^\circ\text{C}$ where f_{nMod} is the subscript for the final modeled temperature in the stage n and f_{nExp} , for the real data.

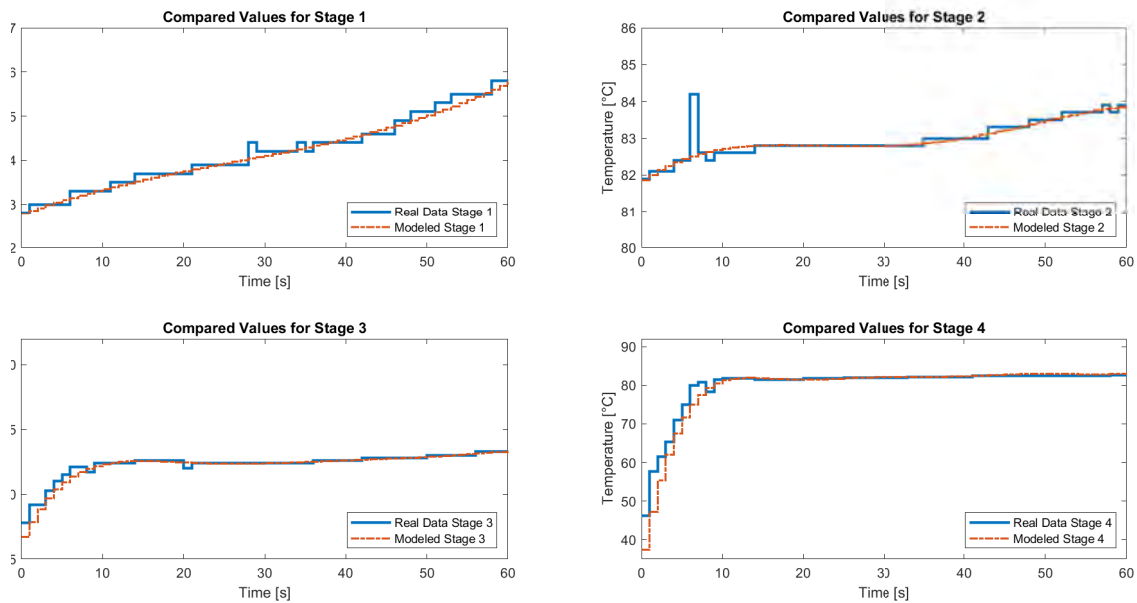


Figure 6.11: Compared Temperatures at stage 1 to stage 4

For the stages 5 to 8, Figure 6.12 shows a comparison between the real temperature data (in blue) and the modeled temperature data (in orange). It can be seen that the model follows well the real data (including the delay given by the vapor rising up along the column) in stages 7 and 8. In stages 6 and, specially, 5 it can be seen that the model follows the data to a degree but also shows differences in the rising slope. This difference is given because in stage 5 is introduced the feed which has its own temperature. However, the impact of the feed temperature only affects the values of the variables in

6.2. Comparison against experimental temperatures

the trays close to it (stages 4, 5 and 6) but will not affect the end product if there is a controller for the reboiler.

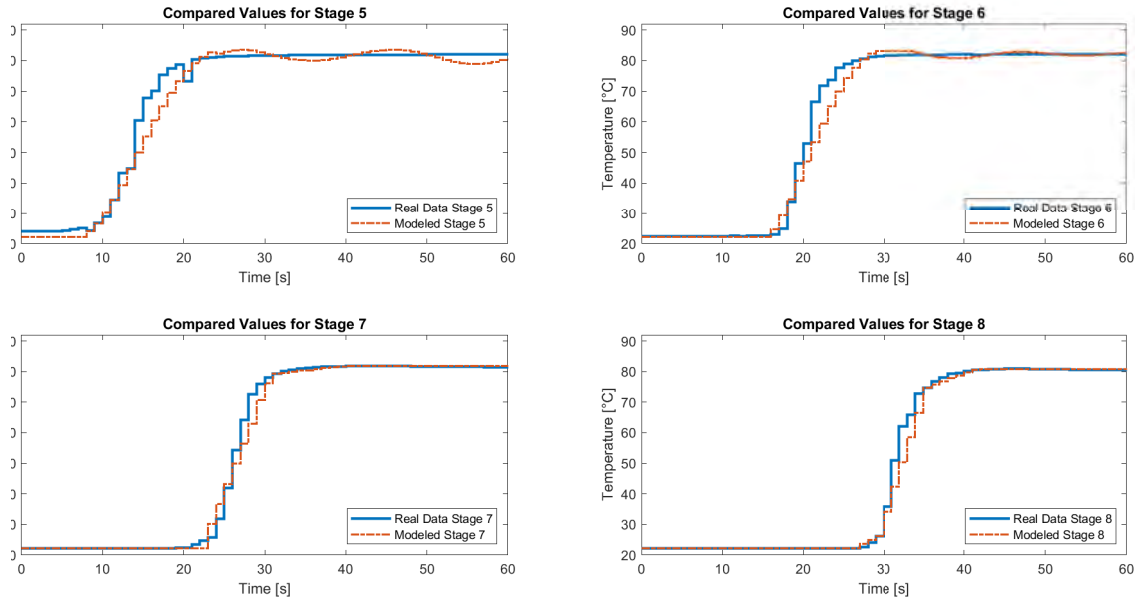


Figure 6.12: Compared Temperatures at stage 5 to stage 8

Finally, Figure 6.13 compares the values for stage 9 and the condenser are shown. The modeled data follows closely the data taken from the experiment, with a maximum error of 12% in the rising curve (at 37 seconds) for stage 9. The final temperatures reach $T_{f10Mod} = 78.5^{\circ}\text{C}$ and $T_{f10Exp} = 78.7^{\circ}\text{C}$, both higher than the ethanol boiling point and lower than the water boiling point. Even with that error, the model is still acceptable since the mean of the error along the mentioned stage is around 0.49°C . In a more rigorous simulation, one should run a series of experiments in order to better characterize the values of the variables of the feed

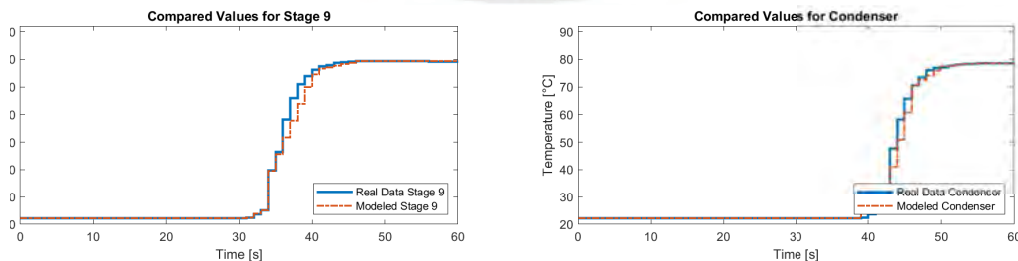


Figure 6.13: Compared Temperatures at Stage 9 and Condenser

The error for the temperature at each stage was calculated and it is shown in Table 6.2. As expected, the bigger errors in temperature are in the middle stages, the ones closer to the feed point. However, the mean of the errors is still small along the column.

Stage	μ_{error}	Maximum Error	σ_{error}
Reboiler	1.7464×10^{-4}	0.307	0.1332
Stage 1	0.052	0.3650	0.1046
Stage 2	0.0319	1.6904	0.2262
Stage 3	0.1041	1.328	0.2797
Stage 4	0.5440	10.5595	2.1469
Stage 5	1.5184	12.6221	3.1346
Stage 6	0.8497	13.1675	2.9980
Stage 7	0.3554	9.6100	2.0114
Stage 8	0.5638	11.6000	2.1694
Stage 9	0.4903	8.1700	1.6312
Condenser	0.2751	7.2000	1.4867

Table 6.2: Temperature error

7 Conclusions and Future Work

This thesis suggested a method to find a theoretical model of a laboratory-scale ethanol-water distillation column, based on **FPM**, located in the Institute of Automation and Systems Engineering at the Technical University of Ilmenau. The objectives of the thesis were to:

1. Investigate system modeling, specifically distillation processes;
2. Develop the theoretical model of the distillation plant;
3. Simulate and improve the model;
4. Compare the model.

For objective 1: Chapter 2 focuses on the background of distillation processes. The concepts reviewed in this chapter include the McCabe-Thiele method, and the relationships and equations given by equilibrium models and thermodynamic properties. And Chapter 3 focuses on the theoretical background of modeling a system, from time series models to the framework for physical modeling.

For objective 2: Chapter 4 provides the mathematical nonlinear model for the mentioned column following the framework for physical modeling from 3.5.

For objective 3: The model found on 4 is simulated in Chapter 5 using Matlab functions and a visual representation made in Simulink using several iterations to get the final variables.

For objective 4: In Chapter 6 the suggested model is compared with the McCabe-Thiele model and with the temperatures measured in the laboratory. The results from the simulations are similar to the values from the McCabe-Thiele diagram and from the

temperature data which indicates the model tend to be correct. However, some clear differences are present specially in stages 5 and 6 since these are the most influenced by the feed stream. And small errors in the vapor phase concentration y at the beginning of the column, also affected by the feed and the initial conditions of the column.

As future work, it will be interesting to use a gas chromatograph (**GC**) in order to, not only determine the actual concentrations and develop a grey-box model, but also to determine the level of contamination inside the plant, like some minerals that may have been introduced along with the water. A future model could also try the model the holdups instead of considering them constants.



Appendix

Appendix A: Ethanol-Water Data

Property	Ethanol	Water
Formula	C_2H_6O	H_2O
Molar Mass	46.069	18.015
Boiling Point	78.2[°C]	99.97[°C]
Gibbs free energy	-168[kJ/mol]	-237.2[kJ/mol]
Specific heat capacity C_v (gas)	1.60[kJ K/kg]	7179.6[kJ K/kg]
Enthalpy of evaporation	42.32[kJ/kg]	40.65[kJ/mol]
Density	997[kg/m ³]	789[kg/m ³]
Critical temperature	243[°C]	373.9[°C]
Standard enthalpy of formation	-241.82[kJ/mol]	-234.8[kJ/mol]

Table 7.1: Ethanol-Water Data [7].

Bibliography

- [1] G. Goodwin. (1999) Control system design. [Online]. Available: https://www.csd.newcastle.edu.au//simulations/dist_sim.html
- [2] C. Schaschke, *A Dictionary of Chemical Engineering*. PAPERBACKSHOP UK IMPORT, 2014. [Online]. Available: https://www.ebook.de/de/product/21333770/carl_schaschke_a_dictionary_of_chemical_engineering.html
- [3] W. L. McCabe and E. W. Thiele, “Graphical design of fractionating columns,” *Industrial and Engineering Chemistry*, vol. 17, no. 6, pp. 605–611, Jun. 1925.
- [4] D. D. BankGmbH. (2021, Jan.) Ethanol water. DDBST GmbH. [Online]. Available: <http://www.ddbst.com/en/EED/VLE/VLE%20Ethanol%3BWater.php>
- [5] J. D. Seader, E. J. Henley, and D. K. Roper, *Separation process principles*. Hoboken, N.J: Wiley, 2006.
- [6] L. Ljung and T. Glad, *Modeling of dynamic systems*. Englewood Cliffs, N.J: PTR Prentice Hall, 1994.
- [7] T. E. ToolBox. (2021, Jan.) Ethanol - thermophysical properties. The Engineering ToolBox. [Online]. Available: https://www.engineeringtoolbox.com/ethanol-ethyl-alcohol-properties-C2H6O-d_2027.html#phases
- [8] R. Luna, F. López, and J. R. Pérez-Correa, “Design of optimal wine distillation recipes using multi-criteria decision-making techniques,” *Computers & Chemical Engineering*, p. 107194, 2020. [Online]. Available: <http://www.sciencedirect.com/science/article/pii/S0098135420312370>
- [9] A. Alkhalabi, “The potential of membrane distillation as a stand-alone desalination process,” *Desalination*, vol. 223, no. 1, pp. 375 – 385, 2008, european Desalination Society and Center for Research and Technology Hellas (CERTH), Sani Resort 22–25 April 2007, Halkidiki, Greece. [Online]. Available: <http://www.sciencedirect.com/science/article/pii/S0011916407008764>

-
- [10] A. Bahadori, "Chapter 12 - liquefied petroleum gas (lpg) recovery," in *Natural Gas Processing*, A. Bahadori, Ed. Boston: Gulf Professional Publishing, 2014, pp. 547 – 590. [Online]. Available: <http://www.sciencedirect.com/science/article/pii/B978008099971500012X>
- [11] G. C. Goodwin, S. F. Graebe, and M. E. Salgado, *Control system design*. Upper Saddle River, N.J: Prentice Hall, 2001.
- [12] F. B. Petlyuk, *Distillation theory and its application to optimal design of separation units*. Cambridge, U.K. New York: Cambridge University Press, 2004. [Online]. Available: www.cambridge.org/9780521820929
- [13] C. Holland, *Fundamentals of multicomponent distillation*. New York: McGraw-Hill, 1981.
- [14] W. Harbert, "System of distillation equations," *Industrial & Engineering Chemistry*, vol. 37, no. 12, pp. 1162–1167, 1945.
- [15] E. Sorel, *Distillation et rectification industrielles*. G. Carré et C. Naud, 1899.
- [16] B. E. Poling, J. M. Prausnitz, and J. P. O'Connell, *The properties of gases and liquids*. New York: McGraw-Hill, 2001.
- [17] W. Luyben, *Process modeling, simulation, and control for chemical engineers*. New York: McGraw-Hill, 1990.
- [18] *Ethanol Plant Development Handbook*, 4th ed., Cotopaxi, Colorado 81223, USA, Jun. 2003. [Online]. Available: <http://www.bbiinternational.com/>
- [19] Y. Peng, X. Lu, B. Liu, and J. Zhu, "Separation of azeotropic mixtures (ethanol and water) enhanced by deep eutectic solvents," *Fluid Phase Equilibria*, vol. 448, pp. 128 – 134, 2017, deep Eutectic Solvents. [Online]. Available: <http://www.sciencedirect.com/science/article/pii/S0378381217301024>
- [20] C. W. Ueberhuber, *Numerical Computation 1*. Springer Berlin Heidelberg, 1997. [Online]. Available: https://www.ebook.de/de/product/14678306/christoph-w_ueberhuber_numerical_computation_1.html
- [21] K. Ogata, *System dynamics*. Harlow: Pearson Education Limited, 2014.
- [22] Y. A. W. Shardt, *Statistics for Chemical and Process Engineers*. Springer-Verlag GmbH, 2015. [Online]. Available: <https://www.ebook.de/de/product/24341390/>

yuri_a_w_shardt_statistics_for_chemical_and_process_engineers.html

- [23] R. E. Kalman, "A new approach to linear filtering and prediction problems," *Transactions of the ASME—Journal of Basic Engineering*, vol. 82, no. Series D, pp. 35–45, 1960.
- [24] E. A. Wan and R. Van Der Merwe, "The unscented kalman filter for nonlinear estimation," in *Proceedings of the IEEE 2000 Adaptive Systems for Signal Processing, Communications, and Control Symposium (Cat. No. 00EX373)*. Ieee, 2000, pp. 153–158.
- [25] P. C. Thijssen, *State estimation in chemometrics : the Kalman filter and beyond*. Cambridge, England Philadelphia, Pennsylvania New Delhi, India: Woodhead Publishing, 2011.
- [26] D. E. Catlin, *Estimation, Control, and the Discrete Kalman Filter*. Springer New York, 2011. [Online]. Available: https://www.ebook.de/de/product/19302581/donald_e_catlin_estimation_control_and_the_discrete_kalman_filter.html
- [27] G. C. G. Juan Yuz, *Sampled-Data Models for Linear and Nonlinear Systems*. Springer-Verlag GmbH, 2013. [Online]. Available: https://www.ebook.de/de/product/21988956/juan_yuz_graham_c_goodwin_sampled_data_models_for_linear_and_nonlinear_systems.html
- [28] G. Goodwin, *Dynamic system identification : experiment design and data analysis*. New York: Academic Press, 1977.
- [29] P. M. Van den Hof, "System identification-data-driven modelling of dynamic systems," *Lecture notes, Eindhoven University of Technology*, February 2012. [Online]. Available: https://venus.tue.nl/ep-cgi/ep_detail.opl?taal=US&fac_id=95&voor_org_id=&rn=19750719
- [30] L. Ljung, *System identification toolbox: User's guide*, 5th ed. 3 Apple Hill DriveNatick, MA 01760-2098: The MathWorks, Inc., 2015. [Online]. Available: <http://www.mathworks.com>
- [31] V. G. KG, *Product Information: Differential pressure transmitter*, Am Hohenstein 113, march 1996. [Online]. Available: <http://www.vega.com/>
- [32] *Freelance 2000, DIGIBROWS*, USA, 2000. [Online]. Available: <https://new.abb.com/products/es/3BDD012601R0101/freelance-2000-digibrows>

- [33] *DigiVis 500: your supervision solution from ABB*, Eppelheimer Strasse 82, 69123 Heidelberg, Germany, 2000. [Online]. Available: <https://abbplc.com/docs/1SBC125036B0201.pdf>

